

The Evolution of Supernovae in Circumstellar Wind-Blown Bubbles I. Introduction and One-Dimensional Calculations.

Vikram V. Dwarkadas

Astronomy and Astrophysics, Univ of Chicago, 5640 S Ellis Ave RI 451, Chicago IL 60637

Submitted to the Astrophysical Journal

`vikram@oddjob.uchicago.edu`

ABSTRACT

Mass loss from massive stars ($\gtrsim 8M_{\odot}$) can result in the formation of circumstellar wind blown cavities surrounding the star, bordered by a thin, dense, cold shell. When the star explodes as a core-collapse supernova (SN), the resulting shock wave will interact with this modified medium around the star, rather than the interstellar medium. In this work we first explore the nature of the circumstellar medium around massive stars in various evolutionary stages. This is followed by a study of the evolution of SNe within these wind-blown bubbles. The evolution depends primarily on a single parameter Λ , the ratio of the mass of the dense shell to that of the ejected material. We investigate the evolution for different values of this parameter. We also plot approximate X-ray surface brightness plots from the simulations. For very small values $\Lambda \ll 1$ the effect of the shell is negligible, as one would expect. Values of $\Lambda \lesssim 1$ affect the SN evolution, but the SN 'forgets' about the existence of the shell in about 10 doubling times or so. The remnant density profile changes, and consequently the X-ray emission from the remnant will also change. The initial X-ray luminosity of the remnant is quite low, but interaction of the shock wave with the dense circumstellar shell can increase the luminosity by 2-3 orders of magnitude. As the reflected shock begins to move inwards, X-ray images will show the presence of a double-shelled structure. Larger values result in more SN energy being expended to the shell. The resulting reflected shock moves quickly back to the origin, and the ejecta are thermalized rapidly. The evolution of the remnant is speeded up, and the entire remnant may appear bright in X-rays. If $\Lambda \gg 1$ then a substantial amount of energy may be expended in the shell. In the extreme case the SN may go directly from the free-expansion to the adiabatic stage, bypassing the Sedov stage. Our results show that in many cases the SN remnant spends a significant amount of

time within the bubble. The low density within the bubble can delay the onset of the Sedov stage, and may end up reducing the amount of time spent in the Sedov stage. The complicated density profile within the bubble makes it difficult to infer the mass-loss properties of the pre-SN star by studying the evolution of the resulting supernova remnant.

Subject headings: circumstellar matter – hydrodynamics – shock waves – supernovae: general – supernova remnants – X-rays: ISM

1. Introduction

Core collapse supernovae (SNe) arise from the collapse of massive stars with mass $M \gtrsim 8M_{\odot}$. As these stars evolve along the main sequence and beyond it, they lose a considerable amount of mass in the form of winds (Kudritzki & Puls 2000). The collective action of the winds from different evolutionary stages may sweep up the material in the ambient medium to form a wind-blown cavity, bordered by a thin, dense, cold shell of material, which contains most of the mass of the swept-up medium. When the star explodes as a SN, the shock wave resulting from the explosion evolves in this highly modified circumstellar medium, and not in the pristine interstellar medium (McKee 1988). The evolution of the supernova remnant is therefore very different from the classical evolution in a constant density interstellar medium, where the remnant successively advances through the phases of free-expansion, adiabatic or Sedov stage, radiative stage and dispersal into the surrounding medium (see for example Woltjer 1972).

Evidence has built up over the last few years that the medium around a pre-SN star is considerably modified by the action of winds, radiation and stellar outbursts. This is highlighted by the famous Hubble Space Telescope picture of the three-ring nebula surrounding the SN 1987A. The combined action of winds and radiation in sculpting this medium is undeniable (Blondin & Lundqvist 1993; Chevalier & Dwarkadas 1995). Other known cases of SNe exploding in wind-driven shells are less spectacular. There are indications that the Cygnus Loop is the remnant of an old supernova explosion that went off in a wind-blown bubble (Levenson et al. 1997). Circumstellar interaction models were earlier proposed for N49 (Shull et al. 1985) and N132D (Hughes 1987). Borkowski et al. (1996) have modeled the X-ray emission from Cas A as arising from a SN explosion within a wind-blown cavity.

Examples of wind-blown bubbles around massive stars are far more numerous (Chu 2003; Cappa et al. 2003). Ring nebulae are seen around main sequence O and B stars, OfPe/WN9 stars (Nota 1999), and many Wolf-Rayet stars in general. Bipolar nebulae are

observed around many LBV stars (Weis 2001), the best-known and studied one being η Carinae (Davidson & Humphreys 1997). Circumstellar nebulae are observed around red supergiant stars such as VY CMa (Smith et al. 2001; Humphreys, Davidson & Smith 2002), and around blue supergiant stars such as NGC6164-5 (Leitherer & Chevarria-K. 1987). The progenitor of SN 1987A is thought to be a blue-supergiant (BSG). A similar structure is seen around the star Sher 25, suggesting that it may be an analogue of SN 1987A (Chu 2003).

The evolution of remnants within wind-blown cavities has merited some attention in the past. The problem was discussed numerically by Ciotti & D'Ercole (1989). It was placed on a firm theoretical footing with analytic calculations by Chevalier & Liang (1989). Early numerical calculations are described in a series of papers by Tenorio-Tagle and collaborators, wherein they discussed the 1-dimensional evolution (Tenorio-Tagle et al. 1990), the 2-dimensional evolution (Tenorio-Tagle et al. 1991), and off-center explosions within pre-existent bubbles (Rozyczka et al. 1993). A review is presented in (Franco et al. 1991). Blondin & Lundqvist (1993) and Martin & Arnett (1995) carried out hydrodynamical simulations of the nebula surrounding SN 1987A, and Chevalier & Dwarkadas (1995) incorporated the effects of the ionizing radiation from the pre-SN star in order to explain the linearly increasing X-ray and radio emission from SN 1987A, as well as the considerable slowing down of the shock front. Borkowski et al. (1996) modeled the X-ray emission from Cas A under the assumption that the SN expanded in a wind-blown bubble.

In recent years the availability of high spectral and spatial resolution data, both space and ground-based, has added considerably to our knowledge of circumstellar (CS) wind-blown bubbles surrounding massive stars. Observations from HST, Chandra, XMM, and now SIRTF have enriched our knowledge of the structure, formation and evolution of wind-blown nebulae. Simultaneously, advances in understanding the structure of the ejected material in supernovae (for e.g. Truelove & McKee 1999; Matzner & McKee 1999) have further increased our understanding of supernova evolution. The worldwide effort gone into studying SN 1987A has enabled us to explore in real time a SN expanding within a wind-blown bubble on its way to becoming a SNR.

The recent confirmation that gamma-ray bursts arise from very massive stars led to the realization that the shock waves in this case may also evolve in the pre-outburst stellar winds from the progenitor, rather than in the ISM. There is some speculation that gamma-ray burst afterglows may be explained in this manner (Chevalier, Li & Fransson 2004). The extreme interest in gamma-ray bursts as cosmological phenomena has given further impetus to the study of supernova shock waves in stellar winds.

Given the considerable increase in our observational knowledge, accompanied by improved theoretical understanding of SN evolution and SN progenitors, we wish to revisit the

evolution of SNRs in circumstellar wind-blown bubbles. We have planned a comprehensive effort to explore the dynamics, kinematics and radiation signatures of SNe expanding in CS wind-blown bubbles. In this first paper we will explore the various aspects of the interaction, define the parameters on which the evolution depends, and carry out a broad parameter survey. Our initial models will be idealized in order to understand the effects of various parameters. In subsequent papers we will take more realistic stellar evolution calculations into account, which provide the wind-properties from a star at each stage. These will help us to explore the structure and kinematics of more complicated objects. Finally we will apply the knowledge gained to investigations of specific astrophysical objects, especially SN 1987A.

The remainder of this paper is organized as follows. In §2 we briefly discuss mass-loss from massive stars. Hot and cool stars are considered separately. In §3 we describe the basic structure of CS wind-blown bubbles, and in §4 we outline the density structure of the ejected SN material. §5 describes a simple analytic solution that helps to understand the basic ideas, and sets the stage for the numerical calculations. A very brief overview of the code is given in §6. In §7 we study the basic features of the interaction of SN shock waves with circumstellar wind-blown bubbles, using spherically symmetric simulations. Two specific cases are chosen to illustrate the basic aspects of the interaction. X-ray brightness profiles and luminosity plots are presented. §8 discusses the implications of our research for the onset and growth of the Sedov stage. Finally, §9 summarizes the basic results, and outlines future work.

2. Stellar Mass Loss

Core-Collapse SNe (which includes the classes Type II, as well as Type Ib/c) arise from the gravitational collapse of massive stars. The line dividing massive versus non-massive stars is usually drawn at about $8 M_{\odot}$, which is the mass at which a star will not eventually turn into a white dwarf (Langer 1994). This however still leaves a large range of stars, with initial main sequence mass between $8 \sim 200 M_{\odot}$, that can explode as SNe. The evolution and mass-loss characteristics of these stars are quite different over this large range. Thus the environment into which a core-collapse SN evolves will be considerably different depending on the initial mass of the star.

The velocity of the wind emitted from a star is generally comparable to or a few times larger than the escape velocity of the star, as would be expected. The mass loss rate depends on what drives the material from the stellar surface (Lamers & Cassinelli 1999). Stars like the sun have coronal, pressure driven winds with a very low mass-loss rate. Hot, luminous stars such as O, B and Wolf-Rayet (WR) stars have radiatively driven winds. The mass-loss mechanism in cool evolved stars, such as red supergiants (RSGs), is not well understood,

although it is suspected to be due to radiation pressure on dust grains.

The two parameters, mass-loss rate and wind-velocity, determine the density of the wind around the star. For a wind with constant properties, the density ρ at a radius r will be given by $\rho = \dot{M}/(4\pi r^2 v_w)$ where \dot{M} is the mass-loss rate and v_w is the wind velocity. In general we can differentiate two clear regimes:

2.1. Mass Loss from cool massive stars:

Most stars larger than about $11 M_\odot$ will become red supergiant stars (Heger 2004). The lack of RSGs above $50-60 M_\odot$ appeared to indicate the existence of an upper limit to the RSG stage. Conflicting reports about this result have been recently clarified by Lamers et al. (2001). More importantly for this paper, most single stars below about $35 M_\odot$ will explode as SNe while in the RSG stage (Heger 2004). These results are quoted only for solar metallicities, for lower metallicities the number of RSGs reduces considerably. Plus rotational mixing, semi-convection and overshoot will change these numbers. Nevertheless, since the number of stars decreases sharply with increasing mass, the result generally implies that a large fraction of core-collapse SNe arise from RSG stars.

While the mass loss process in red supergiants is not generally well understood, they are observed to have very slow winds, on the order of 20-100 km/s, with high mass loss rates on the order of a few times 10^{-5} to $10^{-4} M_\odot/\text{yr}$. The mass loss is not uniform, but could vary over time periods of a few thousand years. One of the best observed post-RSG stars, IRC +10420, shows evidence for an increasingly complex environment around the star, with multiple shells, several individual condensations and a generally asymmetric structure (Humphreys et al. 1997). These authors infer a mass-loss rate about $10^{-6} M_\odot/\text{yr}$ in the main-sequence (MS) phase, increasing to few times 10^{-4} to $10^{-3} M_\odot/\text{yr}$ during various stages of evolution. Another extreme RSG star VY CMa also shows evidence of an asymmetric structure, reflection arcs and knots, and several bright condensations (Smith et al. 2001). The deduced mass-loss rate is about $3 \times 10^{-4} M_\odot/\text{yr}$.

The high mass loss rate and low wind-velocity imply a high density for the circumstellar material around the star. In general the density can be written as:

$$\rho_{RSG} \sim 5 \times 10^{-20} \dot{M}_{-4} r_{17}^{-2} v_1^{-1} \quad (1)$$

where \dot{M}_{-4} is the mass-loss rate in units of $10^{-4} M_\odot$, r_{17} is the radius in units of 10^{17} cms and v_1 is the wind-velocity in units of 10 km/s. Assuming that the RSG stage lasts for 10^5

years, this RSG wind can alter the medium to a distance of a few parsecs.

2.2. Mass Loss from Hot Massive Stars

Stars above about $35 M_{\odot}$ suffer from considerable mass-loss which tends to strip them of their H envelopes. These Wolf-Rayet (WR) stars are presumed to be the progenitors of Type Ib/c SNe, which do not show H lines in their spectrum. These stars are in general hot, massive stars, which lose mass via radiatively driven winds from the stellar surface. Their progenitors are mainly early type O and B stars, with mass-loss rates on the order of 10^{-8} to $10^{-5} M_{\odot}/\text{yr}$, and terminal wind velocities about 1000-3000 km/s (de Jager et al. 1988). When the star evolves off the main sequence stage and into the WR phase (with perhaps some intermediary stages depending on the initial mass), the mass loss rate can increase to a few times $10^{-5} M_{\odot}/\text{yr}$ (van der Hucht 1997). Thus these stars can lose a large fraction of their stellar mass during their lifetime. For example, in one of Norbert Langer's models, a $35 M_{\odot}$ star has only about $9 M_{\odot}$ remaining when it explodes as a supernova, with $26 M_{\odot}$ being deposited in the surrounding medium. This material can form large wind-blown cavities stretching for tens of parsecs. The various evolutionary stages may lead to the formation of multiple wind-blown shells, which may not always be visible.

Given the large wind-velocities of MS and W-R hot stars, the density of the circumstellar medium will be considerably reduced as compared to the RSG stars mentioned above. The density from a W-R wind at a radius r from the star is given by

$$\rho_{WR} \sim 2.5 \times 10^{-23} \dot{M}_{-5} r_{17}^{-2} v_3^{-1} \quad (2)$$

where \dot{M}_{-5} is the mass-loss rate in units of $10^{-5} M_{\odot}$, r_{17} is the radius in units of 10^{17} cms and v_3 is the wind-velocity in units of 10^3 km/s.

It is clear that the density of the wind around a WR star is about 2-3 orders of magnitude less than that around a RSG star. This has important consequences for the SN evolution, since much of the emission from the young remnant is due to the interaction with the circumstellar medium (Chevalier & Fransson 1994). In most cases this depends on the density of the surrounding medium, and will therefore be considerably reduced in a lower-density medium.

The above discussion shows that while SNe arise from both RSG and WR progenitors, the immediate medium into which the shock wave evolves will be quite different. Both of the stages are post-main sequence stages, and the WR stage may sometimes even be a post-RSG

stage. In general the wind from the star in each case will evolve inside a previously evacuated wind-blown cavity carved out by the MS stage. An important distinction however is that the wind from the RSG star is usually slower than the wind from the preceding stage and will not shock it, but will result in a new pressure equilibrium. The fast WR wind will drive a strong shock wave into the surrounding medium. These variations can lead to very different structures around the star.

What is clear is that in many cases a SN will expand into a low-density environment during its initial evolution, with density lower than the surrounding interstellar medium. In the case of SNe from hot massive stars, this low density medium will start right from the star itself. In the case of RSG progenitors, there may exist a very high-density medium around the star, in which the remnant may evolve for a few tens to hundreds of years. Following this the remnant will continue to evolve for some time in a low-density medium formed by the wind from the main-sequence star, usually an O or B star. In this work therefore, we have concentrated on remnants evolving in a low-density circumstellar wind-blown bubble.

2.3. Other Considerations

The evolution of single, massive stars to the supernova stage has received considerable attention. However many stars have one or more companions, the presence of which can considerably alter the evolution of the star. Mass transfer from or to a companion star can slow down or speed up the evolution of the star, alter its evolutionary track, and even result in a stellar explosion as in the case of Type Ia supernovae. The best studied supernova, SN 1987A, is known to have a blue supergiant progenitor, a B3Ia star when it exploded. A blue supergiant progenitor was unexpected, as it indicated that the star on the H-R diagram went from the blue to the red and back to the blue region before it exploded. Although some single-star scenarios have managed to produce a blue supergiant before the star explodes (see for example Woosley et al. 1997), they require very low metallicities. Rotation changes the dynamics somewhat, and may also help to explain the origin of the bipolar circumstellar shell surrounding SN 1987A, but still appears to require special conditions. A BSG progenitor has consequently been suggested as indicative of binary evolution (Podsiadlowski 1992). While conclusive evidence is lacking, it does imply that stars in binary systems evolve differently from single stars, and SN progenitors in binary systems may differ from single-star progenitors. Not surprisingly, the medium around the star will also be correspondingly different. SN 1987A clearly shows the presence of a beautiful bipolar circumstellar shell structure, surrounded by a thin dense shell. However the density within the bubble is neither as large as that in RSGs nor as low as that in W-R stars, but somewhat intermediate between the

two, on the order of 1 particle/cc. A region of ionized wind material, with a density of about 100 particles/cc, also exists inner to the circumstellar nebula (Chevalier & Dwarkadas 1995).

3. Circumstellar Wind-Blown Bubbles

The interaction between the wind from a star and the surrounding medium, be it the ISM or the wind from a previous epoch, can lead to the formation of wind-blown cavities surrounded by a thin, dense, cool shell. The structure of these wind-driven bubbles was first elucidated by Weaver et al. (1977, hereafter W77), and further explored by Koo & McKee (1992a,b). In the simplest case, that of mass-loss from a fast wind with constant parameters interacting with a slower wind (or the ISM) with constant parameters, a self-similar solution can be obtained. Figure 1 shows the pressure and density structure within a wind-blown bubble in this case. Going from left to right we identify four regions a) the freely-flowing fast wind b) the shocked fast wind c) the shocked ambient medium and (d) unshocked ambient medium. An outer or forward shock (R_o) separates the shocked and unshocked ambient medium, and an inner shock, alternatively referred to as a reverse or wind-termination shock (R_t), separates the shocked and unshocked fast wind. The shocked ambient medium is separated from the shocked fast wind by a contact discontinuity (R_{CD}). The example shown is that of an 'energy-conserving' structure. The interior of this structure consists mainly of a low-density, high pressure and therefore high-temperature region. The isotropic pressure of this region is responsible for driving the outer shock wave. The temperature could be high enough to be visible in X-rays, but the emission measure is usually low, so not many bubbles have been observed with present-day X-ray telescopes.

For a wind with constant properties expanding into a constant-density ISM, W77 showed that a self-similar solution could be obtained for the evolution of the contact discontinuity with time, namely $R_{CD} \propto (L_w/\rho)^{1/5} t^{3/5}$. Here L_w is the mechanical wind-luminosity $L_w = 0.5\dot{M}v_w^2$. If the fast wind expands into a slower wind from a previous epoch, the result becomes $R_{CD} \propto (L_w/\rho)^{1/3} t$. Thus the shell expands with constant velocity.

The above description has ignored many other contributing factors. The wind properties are unlikely to be constant throughout the evolution, thus giving rise to multiple shells. UV photons from the hot stars will ionize the medium around the star, thus altering the dynamics. Factors such as conduction and/or magnetic fields may change the interior dynamics. Heat conduction in particular has been cited as one of the reasons for lowering the temperature in the interior of the bubble. Multi-dimensional effects such as hydrodynamic instabilities can alter the evolution (Dwarkadas & Balick 1998), as we shall see in a future paper. The presence of instabilities can result in considerable turbulence within the interior

of the bubble, breaking the approximations of isotropic pressure and a radial velocity field.

The results above refer to a homogeneous medium. In general the ISM is known to be inhomogeneous and clumpy. However (McKee et al. 1984) have shown that an early type main-sequence star may homogenize the medium up to a radius

$$R_h(t_{ms}) = 56n_m^{-0.3} \text{ pc}$$

where $t_{ms} = 4.4 \times 10^6 S_{49}^{-0.25}$ yr is the main sequence lifetime of stars of spectral type B0 to O4, S_{49} is the ionizing flux in units of 10^{49} photons/sec, and n_m is the mean density the cloud gas would have if it were homogenized. Therefore we expect that the medium around an early type star can be treated as a smooth medium at least for distances up to about 50 pc from the star. In later papers we will consider the effects of a clumpy medium.

Thus far we have considered only spherical circumstellar bubbles. The circumstellar structures around many massive stars, especially WR stars and/or Ofpe/W9 stars, do fall in this category. However many nebulae around Luminous Blue Variable (LBV) stars show distinct evidence of bipolarity (Weis 2001). The bipolar structure around SN 1987A has been clearly mapped using light echoes (Crotts et al. 1995). It is unclear what additional ingredients contribute to the formation of these aspherical nebulae. A common explanation tends to invoke an asymmetry in the surrounding medium, such as an equatorial disk, which inhibits the expansion of these nebulae along the equator but allows for free expansion in the polar regions, leading to bipolarity. An alternative explanation attributes the asphericity not to the external medium but to the wind from the star itself. For example a rotating star may give rise to a wind that is faster in the polar regions and slower in the equatorial regions (see for example Dwarkadas & Owocki 2002). In this paper we consider the interaction of SN shock waves with spherical nebulae. In future papers we will consider how the interaction changes due to deviations from sphericity.

It is clear that the circumstellar bubble results from the impact of a fast wind on a slower ambient medium. However in many cases the situation may be reversed, i.e. it is a slower wind that impacts on a faster wind from a previous epoch. This may very well be the general case for RSG winds, whose velocity is about 20 km/s, and which may follow a much faster main-sequence wind. Such a situation is illustrated in Fig 2, which illustrates a snapshot from a simulation in which a MS wind is followed by a RSG wind. The figure shows the density and pressure profiles close to the end of the RSG stage, as the RSG wind creates a new pressure equilibrium. Unlike the case illustrated above, no wind-driven bubble is created, but the wind is almost freely expanding all the way to the interaction region with the main-sequence wind, from which it is separated by a contact discontinuity. The

evolution of the SN ejecta in this medium would be described by the self-similar solutions for power-law ejecta evolving in a power-law ambient medium (see below), up until the time the ejecta collided with the shell. Given the low wind velocity (v_{RSG}) and a maximum RSG lifetime (t_{RSG}) of about 100000 years, the interaction of SN ejecta with a RSG wind can last for about

$$t_{int} = 400 \left(\frac{t_{RSG}}{100,000 \text{ yrs}} \right) \left(\frac{v_{RSG}}{20 \text{ km/s}} \right) \left(\frac{v_{SN}}{5000 \text{ km/s}} \right)^{-1} \text{ years} \quad (3)$$

where we have used an average velocity of 5000 km/s to take deceleration of the ejecta by the dense RSG wind into account. For higher mass-stars the RSG phase may be more short-lived, and the interaction time will decrease. After this period the remnant will continue to evolve in a low-density wind-blown bubble formed by the main-sequence star, until it collides with the dense shell.

4. The SN Ejecta

We are dealing with young supernovae, which are still in an ejecta-dominated stage. To describe the supernova evolution from the early stages, a prescription for the profile of the ejected material is required. This profile is established very early on, in the first few days after the explosion. The velocity of the ejected material tends towards free-expansion, with $v = r/t$ as expected. The density in free-expansion at a particular velocity decreases as t^{-3} (Chevalier & Fransson 1994).

The density distribution of the ejected material depends on the structure of the pre-SN star. In core-collapse SNe where the explosion energy is all contained in the center, the distribution of ejected material depends on whether the envelope is convective or radiative (Matzner & McKee 1999, hereafter MM99), and in the former case on the composition. The radiative case is more typical of W-R stars and other very massive stars, whereas RSGs are better described by the convective case. Analytical and numerical calculations (Chevalier & Soker 1989, MM99) have shown that the ejecta density can be reasonably well represented as a power-law in the outer parts of the ejecta ($\rho_{SN} \propto v^{-n}$), with a flat or shallower distribution ($n < 3$) below a certain velocity v_t . MM99 find that the RSG distribution can be described by a power-law with an exponent $n=11.7$, whereas the convective case is better described by a slightly shallower power law $n=10.2$. We note that these are approximations, although good ones; in general the power-law may vary over the ejecta structure. In fact Dwarkadas & Chevalier (1998) showed by inspection of the numerical models that the ejecta in Type Ia SNe could best be described by an exponential profile.

The interaction of power-law ejecta ($\rho_{SN} \propto v^{-n} t^{-3}$) with a power-law surrounding medium ($\rho_{CS} \propto r^{-s}$) can be described by a self-similar solution (Chevalier 1982), wherein the contact discontinuity evolves with time as $R_{CD} \propto t^{(n-3)/(n-s)}$. Such a formulation has often been used in the past to describe SN evolution in stellar winds.

In this work we assume that the ejecta are described by a power-law, with a power-law exponent of 9. This is close enough to the values suggested by MM99, while also being the value suggested for the ejecta of SN 1987A. The mass of material ejected in the explosion is taken as $10 M_{\odot}$. Our values are different from those used by Tenorio-Tagle and collaborators in all their publications (Tenorio-Tagle et al. 1990). They used a SN density profile decreasing as r^{-3} , and a total mass of ejected material of $4 M_{\odot}$. Their ejecta density profile is too shallow compared to the work of MM99. Besides, a value of $n > 5$ ensures a finite mass and energy for the ejecta. The difference between the density profile used herein and that employed in Tenorio-Tagle et al. (1990) is that their shallower profile results in a considerable amount of the ejected mass being present at large velocities. We have used a higher value for the ejected mass on the assumption that many massive stars, especially in the middle-mass range of $10\text{-}30 M_{\odot}$, would leave behind a compact remnant and eject most of their remaining mass in the explosion. This is an arbitrary number, and in future papers we will compute models with a smaller value of the ejected material. As discussed below, the remnant evolution is not so much a function of the ejected mass itself as of the ratio of the mass of the dense circumstellar shell to the ejected mass. The evolution to the Sedov stage however will depend on the amount of material ejected (see §8).

5. Thin-Shell Model

In this section, we develop an analytical thin shell model for the evolution of the supernova-circumstellar shell interaction. Although some approximations are necessary, the model shows the dependence on the parameters and gives general insight into the evolution.

There are two main approximations. First, the circumstellar shell plus swept-up external gas can be regarded as a thin shell with thickness ΔR much less than radius R . This approximation should be adequate for the early evolution, but will break down as the outer shock front moves away from the shell position. Second, the supernova energy interior to the shell can be regarded as giving a region of constant internal energy. This approximation is inaccurate during the early evolution when there are pressure waves and shock waves moving through the interior, but should become accurate later in the evolution once complete thermalization of the ejecta energy has occurred. A final approximation is that the expansion is spherically symmetric; that is, instabilities do not have a major effect on the evolution.

We consider the circumstellar shell to have a mass M_{sh} and to be surrounded by a cold medium with density distribution $\rho_s = \rho_a(R/R_i)^{-s}$, where ρ_a is a constant, R_i is the initial shell radius, and s is a constant < 3 . The cases of most interest are $s = 0$ (constant density interstellar medium) and $s = 2$ (circumstellar gas from steady mass loss). The mass conservation equation is

$$\frac{dM}{dt} = 4\pi R^2 \rho_s V, \quad (4)$$

where M is the shell mass including the swept up mass and V is the shell velocity. The mass equation can be integrated to yield

$$M = M_{sh}[1 + m(y^{3-s} - 1)], \quad (5)$$

where $m = M_i/M_{sh}$ is a constant, M_i is the mass that the surrounding medium would have if it extended from $r = 0$ to R_i , and $y = R/R_i$.

The shell initially receives an impulse when it is hit by the supernova shock front. CL89 have described some of the details of this interaction, allowing for a steep outer density profile in the supernova ejecta. Here, we make the approximation that the initial shell velocity from this interaction is $V_i = (\alpha p_{sn}/\rho_{sh})^{1/2}$, where α is a constant, $p_{sn} = E/2\pi R_i^3$, E is the supernova energy, and ρ_{sh} is the initial density in the shell. The initial pressure in the shell, p_i , for the shell evolution is then given by $E = 2\pi R_i^3 p_i + M_{sh} V_i^2/2$. We find it convenient to use a dimensionless velocity variable

$$w^2 = \frac{V^2}{mp_i/\rho_a}. \quad (6)$$

With this definition, the initial shell velocity is

$$w_i = \left[\frac{m\rho_{sh}}{\alpha\rho_a} - \frac{1}{(3-s)} \right]^{-1/2}. \quad (7)$$

The equation of motion of the shell is

$$M \frac{dV}{dt} = 4\pi R^2 (p_{int} - \rho_s V^2), \quad (8)$$

where p_{int} is the interior pressure and evolves as $p_i y^{-5}$ due to adiabatic expansion. From the above discussion and substitutions, the equation can be written as

$$\frac{dw^2}{dy} = \frac{2(3-s)y^2(y^{-5} - my^{-s}w^2)}{[1 + m(y^{3-s} - 1)]}. \quad (9)$$

This equation can be solved using standard techniques to give:

$$w^2 = \frac{w_i^2 + (3-s)(1-m)(1-y^{-2}) + 2m(3-s)(1-s)^{-1}(y^{1-s} - 1)}{[1 + m(y^{3-s} - 1)]^2}, \quad (10)$$

where $s \neq 1$. If $s = 1$, such as may occur in a region consisting of molecular clouds (Cernicharo et al. 1985; Stuwe 1990), then we get

$$w^2 = \frac{w_i^2 + 2(m-1)(y^{-2} - 1) + 4m \ln y}{[1 + m(y^2 - 1)]^2}. \quad (11)$$

For completeness, we also show the solution for planar ($q = 1$), cylindrical ($q = 2$), and spherical ($q = 3$) geometry when $s = 0$:

$$w^2 = \frac{w_i^2 + 3 + 6my^{q/3} - 3(1-m)y^{-2q/3} - 9m}{[1 + m(y^q - 1)]^2}. \quad (12)$$

The parameters here have definitions equivalent to those for the spherical case.

The solutions for spherical expansion with $s = 0$ and $s = 2$ are illustrated in Fig 3. The range of m is from 0 (no surrounding medium) to 1 (mass in shell equal to mass external medium would have if it extended from R_i to $r = 0$). The $m = 1$ case is thus what would be obtained if the shell is just the swept-up external medium, as could be the result of a fast wind from the central star sweeping up a slower wind from a previous epoch. The $m = 0$ case would occur, for instance, if the shell were composed of mass ejected from the central star in a low density ambient medium. Low density in this case implies that the mass of any ejected shell is large enough, and the ambient density small enough, that the shocked shell would not sweep up a mass comparable to its own over many doubling times of the radius. Mass ejections on the order of a solar mass have been presumed to occur in Luminous Blue Variables such as η Carinae. If $m = 0$ the shell mass remains constant with time. Strictly speaking the equations (6) and (7) are not valid for $m = 0$, although the final solution in equation (10) still holds. The $m = 0$ cases show little deceleration, but rapid deceleration does occur for higher m . For $s = 0$, it can be clearly seen from equation 10 that for any finite, non-zero value of m , the denominator goes as y^6 for large y . This implies that in the presence of an ambient medium, over several doubling times the shell is invariably going to slow down to a low velocity irrespective of the initial mass and velocity of the shell. It should be kept in mind however that with deceleration the thin shell approximation is expected to break down if the flow is nonradiative.

One way to estimate the deceleration is to examine a “braking index” $\Omega \equiv \ddot{R}R/\dot{R}^2$. For a self-similar flow expanding as $R \propto t^k$, we have $\Omega = (k-1)/k$; the thicknesses of shocked regions for various values of k can be found in (Chevalier 1982). There is a critical value of k corresponding to a point explosion blast wave for which the swept-up shell is expected to become very broad. The value is $k = 2/(5-s)$ or $\Omega_c = -(3-s)/2$. Once this value of Ω is reached, the shock front can be expected to strongly separate from the shell. The braking

index can also be calculated for the shell motion, with the result for the $m = 1$ case:

$$\Omega(s = 0) = -3 \left(\frac{w_i^2 - 6 + 5y}{w_i^2 - 6 + 6y} \right), \quad \Omega(s = 2) = -\frac{w_i^2 + 2 - 3y^{-1}}{w_i^2 + 2 - 2y^{-1}}. \quad (13)$$

We thus find that $\Omega = \Omega_c$ for $y = (6 - w_i^2)/4$ ($s = 0$) and $y = 4/(2 + w_i^2)$ ($s = 2$); the thin shell phase is quite short-lived for $m = 1$. At the other extreme of $m = 0$, there is no deceleration, which is expected because the ambient medium does not exert any significant pressure on the shell, and the shell tends toward a constant velocity. From equation (12), for a spherical shell this occurs when $y^2 \gg 3$.

6. Numerical Simulations

The numerical simulations described herein were carried out using the VH-1 code, a 1,2, and 3-dimensional numerical hydrodynamics code developed by at the University of Virginia by John Hawley, John Blondin et al. It is based on the Piecewise Parabolic Method described in Colella & Woodward (1984). The method is well suited to simulating compressible flows in astrophysics, and the code has been used previously by this author and others for astrophysical calculations. Cooling is employed in the form of a cooling function. We use the one described in Sutherland & Dopita (1993). Cooling is necessary in order to simulate the evolution of the CS bubble and the formation of the thin, dense, cooled shell, but the amount of cooling is relatively insensitive to the details of the cooling function used. Cooling is not generally significant in the evolution of the remnant, except when the shell mass significantly exceeds the ejecta mass (see §7.3). No contact discontinuity steepener is used. Simulations are carried out on a spherical-polar (r, θ) grid. Two-dimensional simulations consider only one quadrant assuming azimuthal and equatorial symmetry. Inflow (describing SN ejecta) and outflow (describing surrounding medium) boundary conditions are used at the inner and outer boundary respectively, while reflecting boundary conditions are used at the remaining boundaries in case of 2D. One advantage of this code is that it employs an expanding grid, which tracks the outer shock front and expands along with it. All grid zones are allowed to expand, and no new grid zones are added (the code is not adaptive). This feature is very useful in simulations where the dimensions of the system change by many orders of magnitude over the evolutionary timescale.

7. Supernova-Circumstellar Bubble Interaction

The structure of the CS bubble as described in §3 consists of a highly evacuated cavity surrounded by a thin, dense shell. When the star explodes as a SN, the shock wave will

interact primarily with a low density medium, with density lower than that of the surrounding ISM. Emission from the remnant arises mainly from the shocked interaction region between the SN shock wave and the ambient medium (Chevalier & Fransson 1994). The low density results in a much lower intensity of emission, since emission at most wavelengths is a function of the square of the density. Thus the emission from the remnant will be considerably reduced compared to an explosion in the ISM, i.e. the remnant will be muffled (McKee 1988). In some cases explosion within a circumstellar bubble made by a hot massive star may render the remnant unobservable until the shock wave impacts the dense circumstellar shell.

The density and pressure profiles within the bubble (Figure 1) show a double-shocked structure separated by a contact discontinuity. When the SN ejecta collide with the freely expanding wind, they drive a strong shock into the wind. A reverse shock is also formed which decelerates the ejecta material. Due to the presence of many shocks and density discontinuities, the subsequent interaction is quite complex, as demonstrated in analytical studies carried out by CL89. In what follows we focus on numerical studies of this interaction.

Most of the mass of the circumstellar bubble is contained in a thin, dense, cool shell bordering the cavity, which suggests that this is the essential parameter influencing the dynamics. This is verified by our simulations and previous work by others (Tenorio-Tagle et al. 1990). The interaction is found to depend on one parameter, the ratio of the mass in the swept-up shell to the mass of the ejected material, which we denote as Λ . If the bubble was formed by the interaction between two winds, then the swept-up mass, and hence Λ , will vary as the radius r (and not r^3 as it would for a constant density surrounding medium).

The role played by the Λ parameter can be understood by comparing to a somewhat analogous situation of an obstruction placed in the path of a body of flowing water such as a river. A small pebble is obviously not going to make much difference. A slightly bigger stone may have an instantaneous impact, but the momentum of the flowing water will quickly overrun it and soon forget that it ever existed. A large boulder which have a much larger impact, and the water, if it is not able to move the stone, will have to flow around it. The flow will be diverted and its velocity altered. And finally if the river is blocked by a dam, the flow will be halted, or at least controlled by the obstruction.

In the same way, $\Lambda \ll 1$ will not have a substantial impact, as the momentum of the ejected material will quickly destroy the pre-existing shell. The impact of the surrounding shell begins to be felt when $\Lambda \lesssim 1$. When $\Lambda \gg 1$ the shell can significantly alter the supernova evolution, speed-up the remnant evolution and perhaps even alter the various phases through which the remnant will evolve.

We illustrate here two cases, Case 1 where $\Lambda \lesssim 1$, and Case 2 where $\Lambda > 1$. In each case

we start with the formation of the bubble by the interaction of two winds. The initial wind was assumed to have a high mass-loss rate ($\dot{M} = 2.5 \times 10^{-5} M_{\odot}/\text{yr}$) and a low wind velocity (50 km/s), analogous to say a RSG wind. The second mass loss phase was assumed to have a slightly lower mass loss rate ($\dot{M} = 8 \times 10^{-5} M_{\odot}/\text{yr}$), but a much larger wind-velocity (2500 km/s), appropriate say for a WR wind. These values are of course arbitrary and vary with each individual case, but they do serve to illustrate the basic point. This assumption is akin to ignoring a main-sequence bubble (although see Case 2 below). This will be an additional ingredient for the future, but the two-wind interaction is simple and sufficient enough to understand the basic characteristics of the SN-bubble interaction. The differences between the bubble in the two cases is due to the different lifetime of each wind phase.

The SN density profile is described by a power-law with exponent $n = 9$. Below a certain velocity, the density is flat in the inner regions. The ejecta mass is uniformly taken to be $10 M_{\odot}$ and the explosion energy to be 10^{51} ergs. The evolution of the SN shock wave into the freely expanding wind is calculated with a high-resolution computation. These two simulations are then mapped onto the grid to form the initial conditions for the SN-CS bubble interaction study.

7.1. Case 1: $\Lambda = 0.14$

We first consider a case where the mass of the wind-swept shell is 14% of the ejecta mass. We assume that this bubble is formed within the interstellar medium i.e. although the medium surrounding the dense shell is a slow wind, we assume that the density of this wind will not fall below that of an ISM density of 1 particle/cc.

Figure 4 shows snapshots from the evolution of the supernova shock-wave within the bubble. The solid lines indicate density, and the dashed lines pressure. R_f indicates the SN shock wave driven into the freely-expanding wind. R_w signifies the wind-termination shock, and R_{sh} the wind-swept shell. The simulation starts at approximately 8.36 years, which is the time that the SN shock has been propagating in the freely expanding wind region of the circumstellar wind blown bubble.

The expanding shock wave collides with the wind termination shock in about 45 years, leading to the formation of a transmitted shock wave that expands into the roughly constant density portion of the wind-blown bubble, and a reflected shock wave that traverses back into the SN ejecta. The collision results in an instantaneous increase in the pressure, as is clearly visible in Fig 4 at time 53.6 years. Note that each time the SN shock wave collides with a shock or density discontinuity, a transmitted and reflected shock wave pair will be

formed. The increased pressure will result in an increased temperature, leading to a rise in X-ray emission following the impact.

The transmitted shock continues to expand in an almost constant density medium until it reaches the wind-blown shell. Meanwhile the reflected shock, which has a high velocity, moves back past the original SN reverse shock and into the SN ejecta. Although the reflected shock is moving backward in a Lagrangian sense, to an external observer the entire system is expanding outwards in radius.

At about 110 years the forward shock (the transmitted shock from the previous stage) collides with the surrounding dense shell. The collision results in a compression of the dense shell, and is again marked by a sharp rise in pressure and therefore temperature, and a dramatic increase in the X-ray luminosity of the remnant (see Figure 7). As illustrated before, the collision results in a transmitted shock (which is not immediately apparent as it takes some time to emerge from the dense shell) and a reflected shock. The high pressure generated by the interaction gives the newly formed reflected shock a much higher velocity than the SN reverse shock. The reflected shock therefore overtakes the reverse shock in its journey back to the center.

The nature of the density profile is of significant interest at this point. As can be seen in Fig 4 at time 247 years, the density decreases as we move outwards in radius from the reflected shock. This will be reflected in the X-ray surface brightness profile. However as the supernova continues to evolve, other factors come into play: over a period of a few doubling times the remnant begins to 'forget' that the interaction ever took place. This will happen when the mass of the swept up material becomes much larger than that of the shell.

At about the same time, the reflected shock reaches the constant density ejecta region. The net effect is that the SN density profile begins to change, as can be clearly seen in Figure 4 at time 1018 years. The density, which was initially *decreasing* from the reflected shock to the contact discontinuity, begins to *increase* from the reflected shock to the contact. By a thousand years this change is clearly visible, although it takes several thousand years before the density profile will completely change and the SN no longer displays any trace of the shell interaction.

It is important that this change be taken into account when computing the emission from the remnant. The changing density profile will substantially alter the appearance of the remnant, as described below. As seen in the last frame of Figure 4, it takes some time for this change to become complete, when the remnant no longer shows any traces of the interaction. In our simulation the reflected shock converges towards the center before this occurs, but the remnant in the last frame of figure 4 is close to this stage.

An interesting point to note is at time 1018 years in figure 4. There is a region just behind the reflected shock, where the *density is decreasing* as we move outwards in radius, whereas the *pressure is increasing*. The opposing density and pressure gradients indicate that this region will be unstable to the Rayleigh-Taylor instability. Our multi-dimensional simulations confirm this suggestion. The instability is of particular importance because it occurs within the remnant, and as the shock moves inwards the unstable region moves in and away from the forward shock. The instability may lead to the formation of clumps and small-scale structure in the interior of the remnant.

The evolution of the radius and velocity of the forward shock are shown in Fig 5. The expansion parameter δ (where $R \propto t^\delta$) is shown in Figure 6. For a SN shock wave with power-law density ejecta evolving in a medium with a power-law density structure, the value of δ is a constant (Chevalier 1982). A constant value of 0.86 is evident in the early part of this simulation, while the shock wave is evolving in the freely expanding wind region. However this behavior changes once the shock wave impacts the wind termination shock, as is readily apparent in Fig 6. A much larger change occurs when the shock impacts the dense wind-blown shell. The velocity of the shock decreases considerably, its radius remains almost constant, and hence the expansion parameter drops precipitously. After the transmitted shock emerges from the shell, it is continually sweeping up interstellar material, and its velocity decreases much faster than within the bubble. As shown in Fig 6 the expansion parameter also gradually decreases. Once the supernova has completely “forgotten” about the interaction and the reverse shock has reached the center, we would expect the supernova to evolve to the Sedov solution. In this case the remnant is just about approaching this value at the end of the simulation.

The current example, and others studied in this paper, correspond to the $m=1$ case in §5, wherein the wind-driven shell is fully composed of swept up material. It is difficult to determine the precise time when the forward shock emerges from the shell, and therefore the precise value of w_i , but it is low. As mentioned in §5, for the $m=1$, $s=2$ case, the shock will separate from the shell by the time the radius of the thin shell has doubled, if not earlier, depending on the initial value of the velocity imparted to the shell. This is clearly visible in Figure 4. The initial radius of the wind-blown shell is just less than a parsec. By the time the remnant is a 1000 years old, the shell radius has more than tripled, and the forward shock can be seen to have already detached from the shell. The velocity profile of the forward shock resembles that for the $m=1$, $s=2$ case (Figure 3), with an initial rise followed by a gradual decline, although the calculation refers to the shell, not the shock wave itself.

A key observation from Fig 6 is that the expansion parameter varies almost continuously with time once the SN shock impacts the wind-termination shock. This behavior can be

contrasted for evolution of the supernova in a wind or constant density medium, where the expansion parameter is a constant for power-law ejecta. The expansion parameter is a quantity that can be measured independent of the distance to an object. It is used to compute the age of the remnant, to discriminate between various models of SNR expansion, and to determine the current phase of expansion. The varying behavior of the expansion parameter within a bubble may cause a problem for such determinations, because what one gets is only an instantaneous value that is not representative of the stage of expansion.

In order to illustrate the changing morphology and appearance of the remnant, as well as the increase in emission due to the shock-shell interaction, we have computed the X-ray emission from the remnant. Figure 7 shows the X-ray luminosity of the system over time. The CHIANTI database was used for this purpose. The X-ray luminosity computed here consists of the free-free and free-bound luminosity, calculated over the waveband 0.2-12.4 Kev. Line emission in X-rays is neglected. This is a good approximation for temperatures above about 3×10^7 K, but lines may be dominant at lower temperatures. Over most of the evolution, the temperature in the shock interaction regions is larger than 10^7 K, and the luminosity calculated here would suffice. Towards the end of the evolution however the temperature, especially that behind the reverse shock, falls below this value, and line emission may be important, in which case our calculation would seriously underestimate the total luminosity.

Almost all the X-ray emission arises from the interaction region between the inner and outer SN shock waves. A major approximation that is made is to assume that the electron temperature is equal to the post-shock temperature computed by the ideal gas law ($T=(\mu m_H/k) P/\rho$). A mean value of μ is used, i.e. no distinction is made between the mean molecular weight of the ejecta and ambient medium. Since these are collisionless shocks, the equilibration time due to Coulomb collisions can be large (a few hundred to thousand years) and therefore the electron and ion populations are not expected to be in equilibrium. Most of the post-shock energy goes into heating the ions. Electrons are subsequently heated by plasma processes that raise the temperature, until temperature equilibration between ions and electrons occurs. Thus it is possible that, especially in the early stages of evolution, the electron temperature is much lower than the ion temperature. In Figure 7 we therefore show two curves for the X-ray luminosity, one using the kinetic temperature (solid line), and one which assumes that the electron temperature is only 10% of the kinetic temperature (dashed line). It is likely that in the early stages the luminosity will start out closer to the lower curve, while as the evolution proceeds the upper curve will be more representative of the actual luminosity.

The qualitative behavior of the two curves is similar, and the main features are seen

in both. In general we note three regions, an initial low-luminosity X-ray region, a sharp increase in the X-ray luminosity when the shock-shell impact takes place, and then a roughly constant high luminosity region following the shock shell impact. The impact results in an increase of almost two to three orders of magnitude in the X-ray luminosity. Although not computed here, a similar rise in luminosity is expected at radio wavelengths. The steep rise in emission and higher luminosity subsequent to the emission are characteristic of shock-shell impact.

In order to illustrate the changing appearance of the remnant, we have also computed approximate X-ray surface brightness profiles to demonstrate the X-ray appearance of the remnant at various times. Since the emission depends on the square of the density and square-root of the temperature, we have computed the integral of this product over the line of sight. This gives us a fair idea of what the X-ray surface brightness profile would look like, up to a normalization factor. All the profiles are normalized to an arbitrary factor, with the same factor being used in both cases, so that the relative intensities can be easily compared. Only emission processes have been included, no attempt has been made to take any absorption into account. Since the intra-cavity density is so low, any absorption of the emission that occurs will happen in the dense shell only.

Figure 8 shows the density profile, and corresponding surface brightness profile, at various times during the evolution. Initially only the SN shock wave is visible in X-rays, as expected. By the time the SN shock reaches the wind-termination shock of the bubble, the X-ray emission from the post-shock region in the low-density ejecta is reduced so much that the wind-blown bubble becomes the dominant X-ray source. The interaction of the SN shock with the wind-termination shock leads to a small spike in the X-ray emission. A much larger jump in X-ray intensity is seen when the SN shock collides with the dense shell, and the transmitted shock emerges. The remnant then appears limb-brightened in X-rays. As the reflected shock traverses the power-law ejecta region, the X-ray emission from the reflected shock also begins to play a major role, and the SN shows a double-shelled appearance in X-rays. However soon after the profile changes due to two factors - the remnant begins to “forget” the interaction, and the reflected shock reaches the inner constant density core of the ejecta. The remnant no longer shows a double-shelled appearance, but shows a decreasing X-ray intensity as we move towards the center of the remnant. Note however that the timescale between frames 5 and 6 is large, a factor of 15 doubling times, which indicates that for a considerably large time the young supernova remnant will show a double-shelled appearance in X-rays. Certainly remnants with a double-shelled appearance in X-rays are not uncommon, one example being Cas A.

7.2. Case 2: $\Lambda = 3.7$

In the second instance we consider a situation where the mass in the swept-up shell is 3.7 times that of the ejecta. The ratio Λ is about 25 times larger than in Case 1. In order to produce a large mass shell we assumed that the wind-wind interaction continues for a very large time, while the surrounding wind density continues to decrease. This implies that the interaction occurs in a lower density medium outside the dense shell, perhaps a pre-existing bubble from a previous stage. The density of the slower wind was allowed to fall to a very low value of about 3×10^{-3} in the simulation, before a floor to the density was set. Note that although this may appear very low, the surroundings of massive stars are complex and very low density regions are not uncommon (McKee 1988). If there was a surrounding main-sequence bubble from a massive star its density could easily be less than 10^{-3} particles/cc.

As the mass of the shell increases relative to that of the ejecta, the energy transmitted by the ejecta to the shell also increases. Thus the SN shock wave can lose a substantial amount of energy upon interaction with the dense shell, and the transmitted shock is correspondingly weakened. The shock wave may also take a larger time to emerge from the shell.

The large shell mass results in a significant increase in pressure as the SN shock impacts the shell. This high pressure behind the reflected shock can result in significantly large velocities for the reflected shock wave, which subsequently expands in a low density medium. The reflected shock can attain very high velocities, and reaches the center in a short time compared to the emergence of the transmitted shock.

Figure 9 shows pressure and density snapshots at various time intervals from a simulation of the evolution of the remnant in this case. As seen from the plot at 112 years, the size of the bubble is much larger than in Case 1. Note also the extremely low density within a large section of the bubble interior, about 0.01 particles/cc. Such low density regions are characteristic of bubbles around main sequence and Wolf-Rayet stars. Although the SN shock wave takes about 2000 years to reach the wind termination shock, due to the low wind density it has not swept up a very large mass of material before that time, and therefore there is hardly any deceleration. The expansion parameter (Fig 11) remains constant at a value of 0.86 until the shock collides with the wind-termination shock, giving rise to the usual double-shocked structure with a reflected and transmitted shock. The transmitted shock then impacts the wind-blown shell (frame 3, 5119 years) again resulting in a reflected and transmitted shock. The impact also imparts considerable momentum to the dense shell, causing the entire remnant to expand outwards. The reflected shock attains high velocities, thermalizing the inner ejecta as it moves towards the center. The transmitted shock, which is expanding into a much higher density medium, moves outwards with much lower velocities.

As expected from the discussion in §5, the forward shock is expected to separate from the shell within a doubling time of the shell. This behavior is illustrated in figure 9, where the shock has detached itself from the shell by the time it has doubled its initial radius. The velocity profile resembles that for a decelerating shock wave that is slowing down as it sweeps up more material.

By about 20,000 years the reflected shock has converged onto the center. A weak re-reflected shock is formed that expands outwards. The impact of this shock with the dense shell does not result in an appreciable increase in the X-ray luminosity. Unlike Case 1, in this case the reflected shock reaches the center before the transmitted shock has separated itself significantly from the shell, and the system does not easily “forget” the interaction.

It can be seen that although the remnant is almost 50,000 years old by the end of the simulation, it does not yet display the profile characteristic of the Sedov adiabatic stage. In particular, even after the reflected shock has converged on the center and a weaker re-reflected shock is present, the system is dominated by only the forward shock wave, but the density profile is still different from the Sedov solution. This illustrates an important characteristic of SNRs evolving in low-density wind-blown bubbles - the evolution may deviate from the classical description of ejecta-dominated, Sedov and radiative stages.

When the reflected shock is moving towards the center, almost the entire interior of the remnant is very hot, about 10^8 degrees. If the density in the interior is high enough, the emission measure will be large and the entire remnant will be visible in X-rays. In the current example this is not the case, as the interior density is quite low. But it is possible to envisage a situation where the shock-shell interaction occurs earlier in the remnant’s evolution (such as Case 1) but the wind-blown shell still has mass larger than the ejecta. Then the reflected shock will traverse much higher density ejecta on its way to the center, and the emission from behind the reflected shock could be comparable to that from the forward shock. The surface brightness profile would then show X-rays all the way to the center. It is possible that such an effect could be one explanation for the so-called mixed-morphology remnants, which are X-ray bright all the way to the center.

Figure 10 shows the radius and velocity evolution of the forward shock in this case, and Figure 11 is a plot of the expansion parameter evolution. In both cases they resemble closely the counterparts in Case 1. The expansion parameter remains constant up to the SN-wind termination shock interaction, then a slight decrease until the shock-shell impact takes place, followed by a significant decrease in the velocity and expansion parameter. As the transmitted shock emerges the expansion parameter increases again, and then gradually decreases till it approaches the Sedov value of 0.4 in a constant density medium. It is clear that even though the behavior of the reflected shock and the interior structure of the remnant

is quite different in both cases, this is not reflected in the behavior of the outer shock. This serves as a cautionary note that studying the behavior of the outer shock is not sufficient to provide information regarding the evolutionary phase and structure of the remnant.

Figure 12 shows the X-ray luminosity of the remnant over time. The overall evolution is similar to that in case 1, although the increase in X-ray luminosity upon impact is smaller. In this case the density is generally very small, and the temperature high enough that line-emission is not important over almost the entire evolution. The X-ray luminosity is much lower in the beginning, given the low density of the bubble interior. It is unlikely that such a remnant could be observed by available X-ray instruments. The luminosity jumps upon shock-shell impact. However the overall level is a couple of orders of magnitude lower than in Case 1.

Fig 13 shows the approximate X-ray surface brightness profiles, similar to Figure 8. Again we start out with the SN shock being the most visible source of X-rays. The interaction of the SN shock wave with the wind-termination shock leads to the expected rise in X-ray emission, and the interaction with the wind-blown shell results in an even larger jump in the x-ray intensity. Up to this point the X-ray evolution is similar to the previous case. Beyond this however it departs considerably, because the reflected shock does not have much time to interact with the power-law ejecta before reaching the constant density inner core. Therefore the remnant never takes on a double-shelled appearance, but the major X-ray emitting region is always the outer transmitted shock. As the reflected shock moves in the entire remnant may be bright in X-rays. In the current case the emission measure is low enough that the remnant may not be observable. But if the shock-shell interaction happens early enough, then this is a possibility worth investigating.

The reflected shock reaches the inner boundary before the transmitted shock has advanced significantly. On reaching the center a re-reflected shock is formed. This is expected in a realistic situation when a spherical shock wave converges onto a compact object. Note that the shock reflected off the boundary is quite weak, and is not readily visible in X-rays (frame 6).

7.3. $\Lambda \gg 1$

In some cases the shell mass may be considerably larger than the ejecta mass. This can happen for instance if a massive star sheds a large amount of mass during its evolution, leading to a pre-SN star with a considerably smaller mass than the main-sequence value. Stars with initial mass greater than about $40 M_{\odot}$ may end up with pre-SN masses of $10 M_{\odot}$

or less. In some cases it is possible that the mass of the wind-blown shell is considerably larger than that of the ejected material, and $\Lambda \gtrsim 25$. In such extreme cases, when the SN shock wave collides with the shell it will impart a considerable fraction of the explosion energy to the shell. The shock wave then becomes radiative, its velocity decreases considerably and the time taken to emerge from the dense shell becomes extremely large. In the limit that the shock loses most of its energy to the shell, only a very weak transmitted shock will emerge from the shell. The SN has then gone from the free-expansion phase to the radiative phase, completely bypassing the Sedov phase. The reflected shock will be quite strong and will thermalize the ejecta in a much shorter time. The dense shell will expand with the additional energy imparted to it, but the SN shock wave will not be visible as a separate entity ahead of the dense shell. This case has been discussed in detail by Tenorio-Tagle et al. (1990).

Such cases, although not common, are quite plausible. Many WR nebulae have masses that exceed 25-30 M_\odot . Cappa et al. (2003) list some WR nebulae with masses of hundreds to thousands of solar masses, mostly made up of swept-up material. When the star explodes as a SN in these nebulae the value of Λ could be very large, possibly 50-100. In these cases the nebula will confine the SNR, and the remnant will never emerge from the nebula. The size and dynamics of the remnant are limited by that of the nebula, whose size is essentially set by mass-loss in the main-sequence phase.

8. Discussion

It is clear that the medium around the progenitor star plays a large role in shaping the further evolution of the remnant. Depending on the nature of the progenitor star, the density of the medium into which the SN shock expands may vary considerably. RSG progenitors will have a region of very high density, surrounded by a low-density bubble formed by the main-sequence star, bordered by a dense shell. WR progenitors will have a low density wind-blown bubble surrounding the star, bordered by a dense circumstellar shell. The interior of the shell may show density variations depending on the various stages of evolution prior to the SN stage. As we have seen in the case of SN 1987A, BSG progenitors will form a cavity with density somewhat midway between the above two cases. Factors such as ionization, rotation, binary evolution and magnetic fields could all affect these results.

Quite often the SNR spends a not insignificant fraction of its life within the bubble. It is then of interest whether the SN reaches a Sedov stage while inside the bubble or not. Note that, depending on the density profile, the swept-up mass must be several times that of the ejecta mass before the remnant enters the Sedov stage (see for example Dwarkadas

& Chevalier 1998). Whether the remnant sweeps up enough material is a function of the ejected mass and the bubble interior density. The bubble density depends on the nature of the exploding star, which is a function of its initial mass and mass-loss rate. If the density into which the SN shock evolves is very low, then the remnant will not sweep up much material, and will remain in the free-expansion phase for a much longer time than it would in the ISM. This is probably the case with WR progenitors. For remnants expanding in a low-density bubble it is unlikely that they will reach the Sedov stage before they collide with the dense shell. As mentioned in §7.3 in cases where the mass of the shell significantly exceeds that of the ejecta, the remnant may evolve from the free-expansion stage directly to the radiative stage, completely bypassing the Sedov stage.

If the progenitor is a RSG, then the surrounding density could be much higher than that of the ISM. The remnant will sweep up a large mass of material in a short time. Whether it evolves to the Sedov stage then depends on the mass of the ejected material and the size of the RSG wind-region, which depends primarily on the time spent in the RSG stage. It is likely that the dense RSG wind will be surrounded by a low density main-sequence bubble, whose density could be a few orders of magnitude lower than that of the RSG wind. If the remnant has already reached the Sedov stage then the evolution will continue as a Sedov-type blast wave in a low density medium. If the remnant has not reached the adiabatic stage then it is unlikely that it will do so in the much lower density medium, and it will probably continue to be in free-expansion until the shock wave collides with the circumstellar shell.

The ejecta mass depends on the initial (zero-age main sequence) mass of the star, the mass of the progenitor star just prior to the explosion, and the nature of the compact stellar remnant. All of these factors depend on the metallicity. According to recent work by Heger et al. (2003) and Woosley et al. (2002), stars in the mass range between 10 and 25 M_{\odot} and solar metallicity will leave behind a neutron star, and will have an ejecta mass about 10 solar masses or larger. However much more massive stars can form larger mass black holes, and the ejecta mass is reduced to just a few solar masses. A very broad conclusion that can be drawn is that RSG stars will result in a large ejecta mass, whereas WR stars will have a much lower ejecta mass (this is not true for stars between 25 and 35 M_{\odot}). As we discussed before SNe from WR progenitors will evolve in a much lower density medium than those from RSG progenitors. Thus larger (smaller) ejecta mass SNe will evolve in denser (low density) winds. A general conclusion is that it will be difficult in most cases for the SNR to sweep up enough material to reach the Sedov stage before colliding with the dense shell.

The situation is opposite for SNe whose progenitor stars lie between about 25 and 35 M_{\odot} , which will explode as RSGs but leave behind a black hole with mass much larger than that of a neutron star, and a very small mass of ejected material. These stars will most

likely be surrounded by a higher-density medium, and therefore will tend to reach the Sedov stage quickly. When this Sedov remnant collides with the dense shell, the reflected shock will traverse an almost evacuated medium and move very quickly back to the center.

In higher mass stars the situation will be further complicated. The WR stage is a highly evolved stage of a high-mass star greater than about $35 M_{\odot}$. It is likely to be preceded by a RSG stage or perhaps even a Luminous Blue Variable (LBV) stage, if the initial mass of the star is much larger (Langer et al. 1994). LBVs can have very large mass-loss rates, and therefore very high-density winds, even compared to RSGs. What this implies is that the WR stage will generally follow a phase of very high-density winds. The WR phase itself has a high mass-loss rate and wind velocity. The momentum of the WR wind is generally going to be much larger than the RSG wind, and may even exceed that of the LBV wind, although this depends on the specific parameters. If the WR wind was preceded by a low-velocity RSG wind, the WR wind momentum will carry the RSG wind material along with it. This combined material may collide with the main sequence shell and reflect back, forming more complicated structures than described herein. The low density WR wind may end up containing higher-density material from the RSG stage. The density profile will not be representative of the wind-properties of the pre-SN progenitor star.

It is apparent that the medium into which a core-collapse SN evolves cannot be easily categorized into either a constant density medium such as the ISM, or a wind with a density $\rho \propto r^{-2}$. A wind-blown bubble formed by two-wind interaction includes both elements, a density that decreases as r^{-2} followed by a more-or less constant density region between the wind termination shock and the contact discontinuity. However in stars larger than $35 M_{\odot}$ mass-loss in the various evolutionary stages preceding the SN explosion can give rise to very complicated density profiles beyond the wind-termination shock. Close in to the star the density generally follows a $1/r^2$ law resulting from the last phase of evolution, but further beyond the density may vary considerably depending on the evolutionary sequence. These more realistic structures will be the subject of future papers.

9. Summary

In this paper we have studied the evolution of supernova shock waves in the circumstellar structures formed by pre-supernova mass loss. The evolution depends mainly on one parameter Λ , the ratio of the mass of the dense surrounding shell to the mass of the ejected material. We have explored the changes in the evolution as the value of this parameter increases, and found that the evolution is significantly different from that for an explosion in the interstellar medium. In particular as the value of Λ increases we find that the en-

ergy imparted to the shell increases, the evolution of the remnant is speeded up, and the appearance of the remnant may change.

In contrast to the work of Tenorio-Tagle et al. (1990, hereafter TBFR90), we have used a much steeper density profile for the outer ejecta and a higher ejecta mass. We have also explored more thoroughly the region around $\Lambda \sim 1$, using two different values of $\Lambda = 0.14$ and $\Lambda = 3.7$. Simulations were also carried out, although they are not explicitly reported herein, with $\Lambda \gg 1$. Our results are consistent with the work of TBFR90 for $\Lambda \gg 1$, as would be expected. However, unlike TBFR90, we have explored two different cases around the value $\Lambda \sim 1$ and find considerable difference between the two cases. These differences can be noted in the evolution as well as the X-ray appearance. In one case a double-shelled structure is visible for a considerable amount of time after the shock shell interaction. In the other case the double shell is mostly absent, but if the interior density is high the entire remnant may be visible in X-rays. However differences are not so easily apparent in observations of the forward or outer shock front. Thus we caution that inferring the properties simply by observing the outer shock parameters can often lead to erroneous conclusions.

We have presented the evolution of the expansion parameter in each case. It is worth pointing out again that the expansion parameter varies significantly over the evolution, unlike in the case of explosion within a constant density medium or a wind. This is very important, because it implies that any instantaneous value of the expansion parameter is not representative of the evolutionary stage of the remnant, and will lead to an incorrect determination of properties. And in particular, assuming that the remnant is in the Sedov stage for computing the remnant parameters could lead to large errors.

The initial evolution of the bubble, within a low-density medium, can result in a large amount of time spent in the free-expansion phase, as the swept-up mass remains quite small. The presence of the circumstellar shell on the other hand, results in significant deceleration of the SN shock wave, and decreases the time spent in the Sedov stage as compared to the radiative stage. The net result is that the Sedov stage could be significantly shortened, and in some cases (see §7.3) may be entirely by-passed. It is plausible however that the forward shock, after emerging from the CS shell, may reach the Sedov stage. It is also quite likely though that given the deceleration of the shock front, which we have seen will occur even when the shell mass is about 10% of the ejecta mass, that the remnant may still reach the radiative stage much faster than in the absence of the shell.

Our X-ray profiles show that for $\Lambda \lesssim 1$, a double-shelled structure is seen in X-rays, with emission coming mainly from shocked shell and from behind the reverse shock. It is possible that such a situation is present in Cas A. At later times when the outer shock has separated significantly from the shell, the emission from the outer shock begins to predominate. In

the case with larger Λ the emission from the shocked shell always seems to predominate. It is clear then that as the remnant evolves and the outer shock separates, the X-ray emission from the shocked shell will appear to come from deep within say the radio emission arising from behind the outer shock. Precisely such a situation has been surmised for the remnant W44 (Koo & Heiles 1995).

In this paper we have not considered multi-dimensional effects such as hydrodynamical instabilities and turbulence. These aspects will be dealt with in upcoming papers. Thin shells are known to be unstable, due to many instabilities ranging from the well-known Rayleigh-Taylor and Kelvin-Helmholtz type, to the range of instabilities lumped under the heading of Vishniac-type instabilities. These instabilities may cause the shells to fragment, and lead to hydrodynamic behavior that has not been explored herein. Furthermore, variations in pressure can lead to turbulent behavior within the interior of the dense shells. Also of significance is that, as the reflected shock in Case 1 moves back to the center, there is a region behind the reflected shock that is Rayleigh-Taylor unstable. This instability is of importance because it occurs in the interior of the remnant, far away from the dense shell and forward shock, and can result in ejecta clumps and filaments in the inner regions of the remnant.

Finally, the real test of these results will be to compare and validate them with observed SNRs. We are indeed fortunate to be able to closely witness the formation and evolution of a SN which occurred within a wind-blown bubble, SN 1987A. The enormous body of observational data that has been collected should enable us not only to study this SN in the utmost detail, but by extension should provide considerable information on the general theory of SN evolution in wind-blown cavities. Of course SN 1987A has its own share of complexities, and a thorough understanding of the circumstellar medium requires 3-dimensional radiation hydrodynamics modeling, which has not yet been carried out. Specific comparisons between our models and observed remnants will be described in later papers in this series.

Vikram Dwarkadas is supported by award # AST-0319261 from the National Science Foundation. This work was initially started as part of my PhD thesis, and it is a pleasure to acknowledge the collaboration and guidance of Roger Chevalier at the University of Virginia, who first encouraged me to work on this topic. I also thank Roger for a careful reading of the paper. I am grateful to Chris McKee for extremely stimulating discussions and helpful suggestions. Suggestions from Bob Rosner, Kris Davidson and Roberta Humphries are gratefully acknowledged.

REFERENCES

Blondin, J. M. & Lundqvist, P. 1993, *ApJ*, 405, 337

Borkowski, K., Szymkowiak, A. E., Blondin, J. M. & Sarazin, C. L. 1996, *ApJ*, 466, 866

Cappa, C. E., Arnal, E. M., Cichowski, S., Goss, W. M., Pineault, S, in “A Massive Star Odyssey: From Main Sequence to Supernova”, IAUS 212, Eds. K. A. van der Hucht, A. Herrero, & C. Esteban, SF: ASP, 596

Cernicharo, J., Bachiller, R., & Duvert, G. 1985, *A&A*, 149, 273

Chevalier, R. A., Li, Z.-Y., & Fransson, C. 2004, *ApJ*, 606, 369

Chevalier, R. A. & Dwarkadas, V. V. 1995, *ApJ*, 452, L45

Chevalier, R. A. & Fransson, C. 1994, *ApJ*, 420, 268

Chevalier, R. A. & Liang, E. P. 1989, *ApJ*, 344, 332

Chevalier, R. A. & Soker, N. 1989, *ApJ*, 341, 867

Chevalier, R. A. 1982, *ApJ*, 258, 790

Chu, Y.-H. 2003, in “A Massive Star Odyssey: From Main Sequence to Supernova”, IAUS 212, Eds. K. A. van der Hucht, A. Herrero, & C. Esteban, SF: ASP, 585

Ciotti, L., & D’Ercole, A. 1989, *A&A*, 215, 347

Colella, P., & Woodward, P. R. 1984, *J. Comput. Phys.*, 59, 264

Crotts, A. P. S., Kunkel, W. E., & Heathcote, S. R. 1995, *ApJ*, 438, 724

Davidson, K. & Humphreys, R. M. 1997, *ARA&A*, 35, 1

de Jager, C., Nieuwenhuijzen, H., & van der Hucht, K. A. 1988, *A&ASupplement*, 72, 259

Dwarkadas, V. V., & Owocki, S. P. 2002, *ApJ*, 581, 1337

Dwarkadas, V. V., & Chevalier, R. A. 1998, *ApJ*, 497, 807

Dwarkadas, V. V., & Balick, B. 1998, *ApJ*, 497, 267

Franco, J., Tenorio-Tagle, G., Bodenheimer, P., & Rozyczka, M. 1991, *PASP*, 103, 803

Heger, A. 2004, private communication

Heger, A., Fryer, C. L., Woosley, S. E., Langer, N., & Hartmann, D. H. 2003, *ApJ*, 591, 288

Hughes, J. P. 1987, *ApJ*, 314, 103

Humphreys, R., Smith, N., Davidson, K., Jones, T. J., et al. 1997, *AJ*, 114, 6

Humphreys, R., Davidson, K., & Smith, N. 2002, *AJ*, 124, 1026

Koo, B.-C., & Heiles, C. 1995, *ApJ*, 442, 679

Koo, B.-C., & McKee, C. F. 1992a, *ApJ*, 388, 93

Koo, B.-C., & McKee, C. F. 1992b, *ApJ*, 388, 103

Kudritzki, R.-P., & Puls, J. 2000, *ARA&A*, 38, 613

Lamers, H. J. G. L. M., Nota, A., Panagia, N., Smith, Linda J., & Langer, Norbert 2001, *ApJ*, 551, 764

Lamers, H. J. G. L. M., & Cassinelli, J. 1999, *Introduction to Stellar Winds*, CUP.

Langer, N., Hamann, W.-R., Lennon, M., Najarro, F., Paudlach, A. W. A., Puls, J. 1994, *A&A*, 290, 819

Langer, N. 1994, in “Circumstellar Media in the Late Stages of Stellar Evolution”, Proceedings of the 34th Herstmonceaux conference, eds. R.E.S. Clegg, I. R. Stevens & W. P. S. Meikle, Cambridge: CUP, 1

Leitherer, C. & Chavarria-K., C. 1987, *A&A*, 175, 208

Levenson, N. A. et al., 1997, *ApJ*, 484, 304

MacDonald, J., & Bailey, M. E. 1981, *MNRAS*, 197, 995

Martin, C. L., & Arnett, D. 1995, *ApJ*, 447, 378

Matzner, C. D. & McKee C. F. 1999, *ApJ*, 510, 379

McKee, C. F. 1988, in “Supernova Remnants and the Interstellar Medium”, Proceedings of IAU Colloquium 101, eds. R. S. Roger & T. L. Landecker, Cambridge: CUP, 205

McKee, C. F., van Buren, D., & Lazareff, B. 1984, *ApJ*, 278, L115

Nota, A. 1999, in “Variable and Non-spherical stellar winds in Luminous Hot Stars”, IAU Coll 169, eds. B Wolf, O Stahl and S. W. Fullerton, Berlin: Springer, 62

Podsiadlowski, P. 1992, PASP, 104, 717

Rozyczka, M., Tenorio-Tagle, G., Franco, J., & Bodenheimer, P. 1993, MNRAS, 261, 674

Shull, P., Jr., Dyson, J. E., Kahn, F. D., & West K. A. 1985, MNRAS, 212, 799

Smith, N., Humphreys, R. M., Davidson, K., Gehrz, R. D., Schuster, M. T., & Krautter, J. 2001, AJ, 121, 1111

Stüwe, J. A. 1990, A&A, 237, 178

Sutherland, R., S., & Dopita, M. A. 1993, ApJS, 88, 253

Tenorio-Tagle, G., Rozyczka, M., Franco, J., & Bodenheimer, P. 1991, MNRAS, 251, 318

Tenorio-Tagle, G., Bodenheimer, P., Franco, J., & Rozyczka, M. 1990, MNRAS, 244, 563

Truelove, J. K., & McKee, C. F. 1999, ApJS, 120, 299

van der hucht, K. 1997, Ap&SS, 251, 311

Weaver, R., McCray, R., Castor, J., Shapiro, P., & Moore, R. 1977, ApJ, 218, 377

Weis, K. 2001, RvMA, 14, 261

Woltjer, L. 1972, ARA&A, 10, 129

Woosley, S. E., Heger, A., & Weaver, T. A. 2002, RMP, 74, 1015

Woosley, S. E., Heger, A., Weaver, T. A., & Langer, N. 1997, to appear in 'SN 1987A: Ten years after', Eds. M.M. Phillips and N.B. Suntzeff, PASP

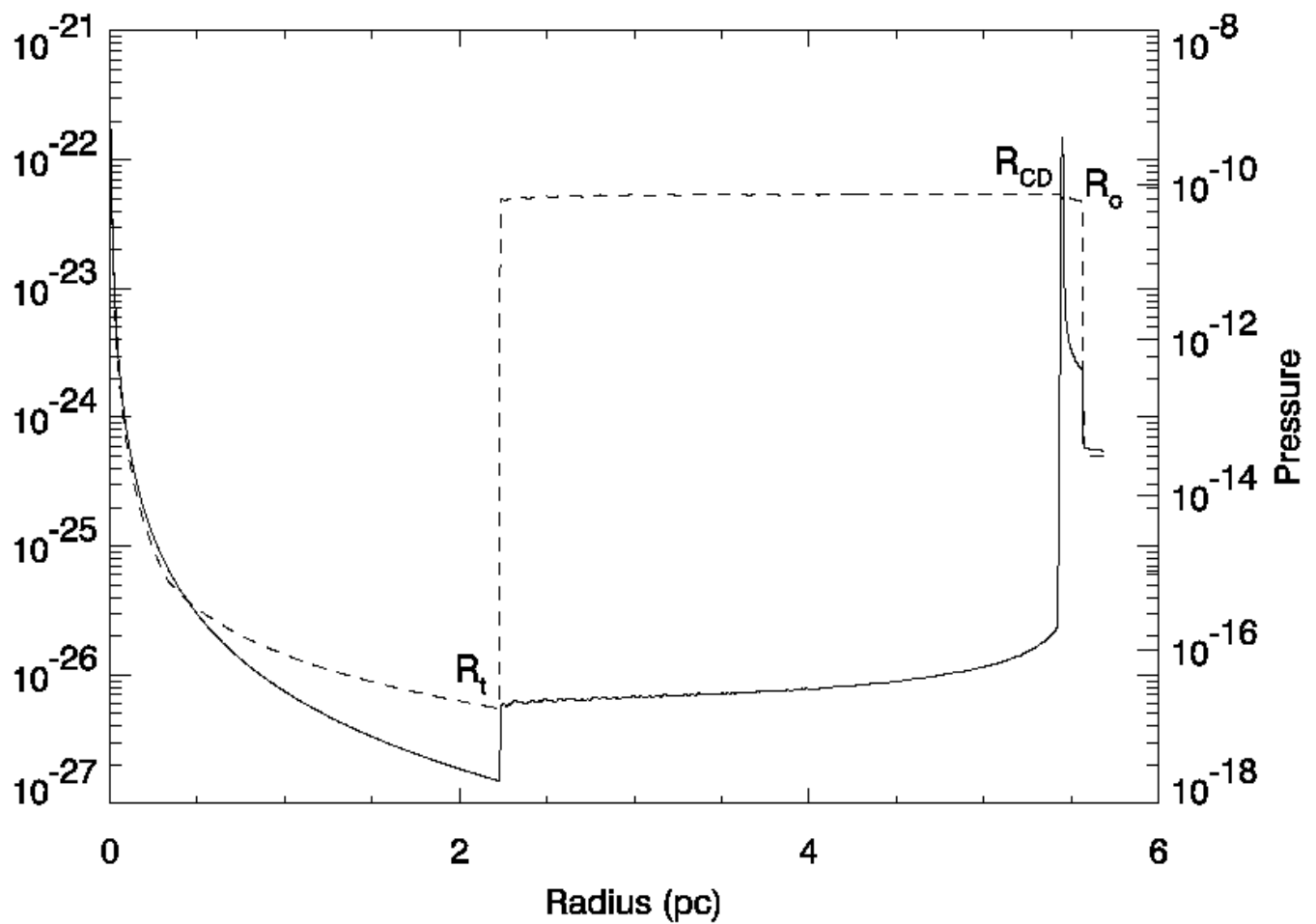


Fig. 1.— Density (solid) and Pressure (Dashed) profiles showing the structure of a wind-blown bubble. R_t refers to the wind-termination shock, R_o to the outer shock, and R_{CD} to the radius of the contact discontinuity.

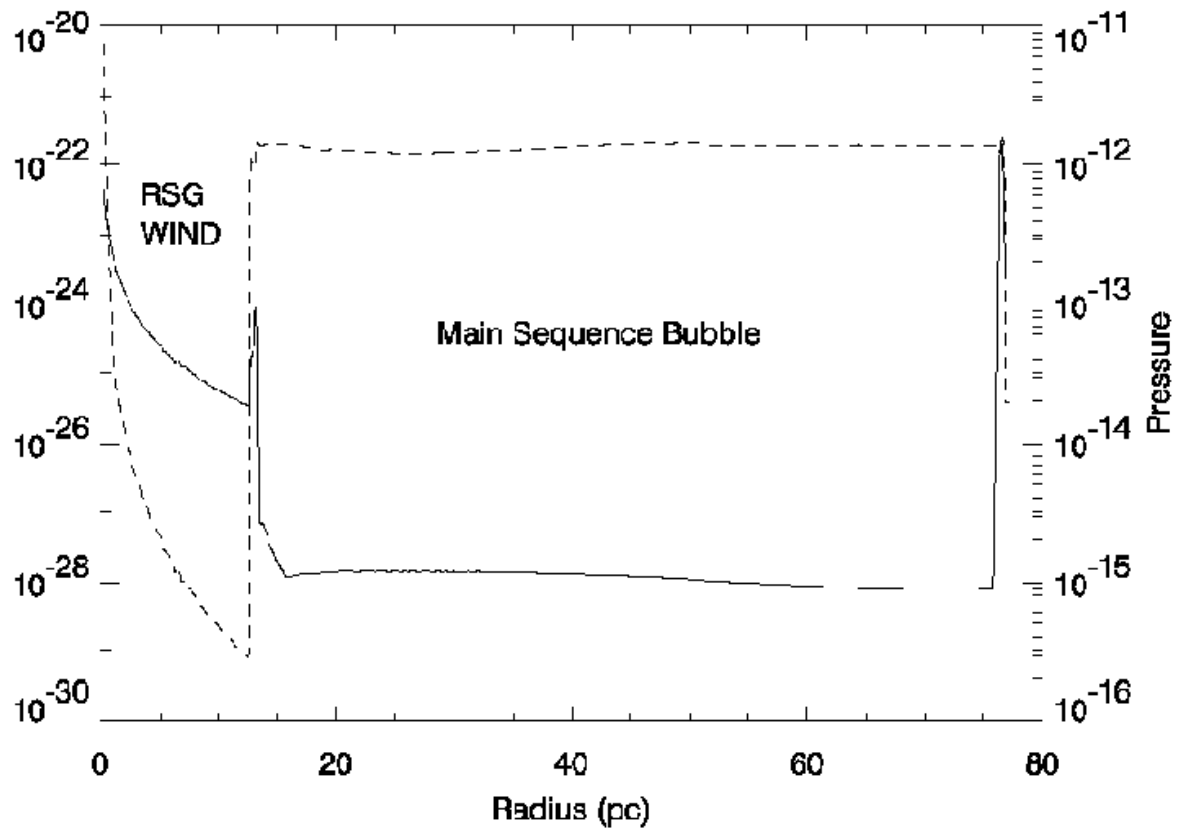


Fig. 2.— Density (solid) and Pressure (Dashed) profiles for the medium around a RSG star. The main-sequence wind formed a wind-blown bubble around the star, whereas the subsequent very high density RSG wind created a new pressure equilibrium.

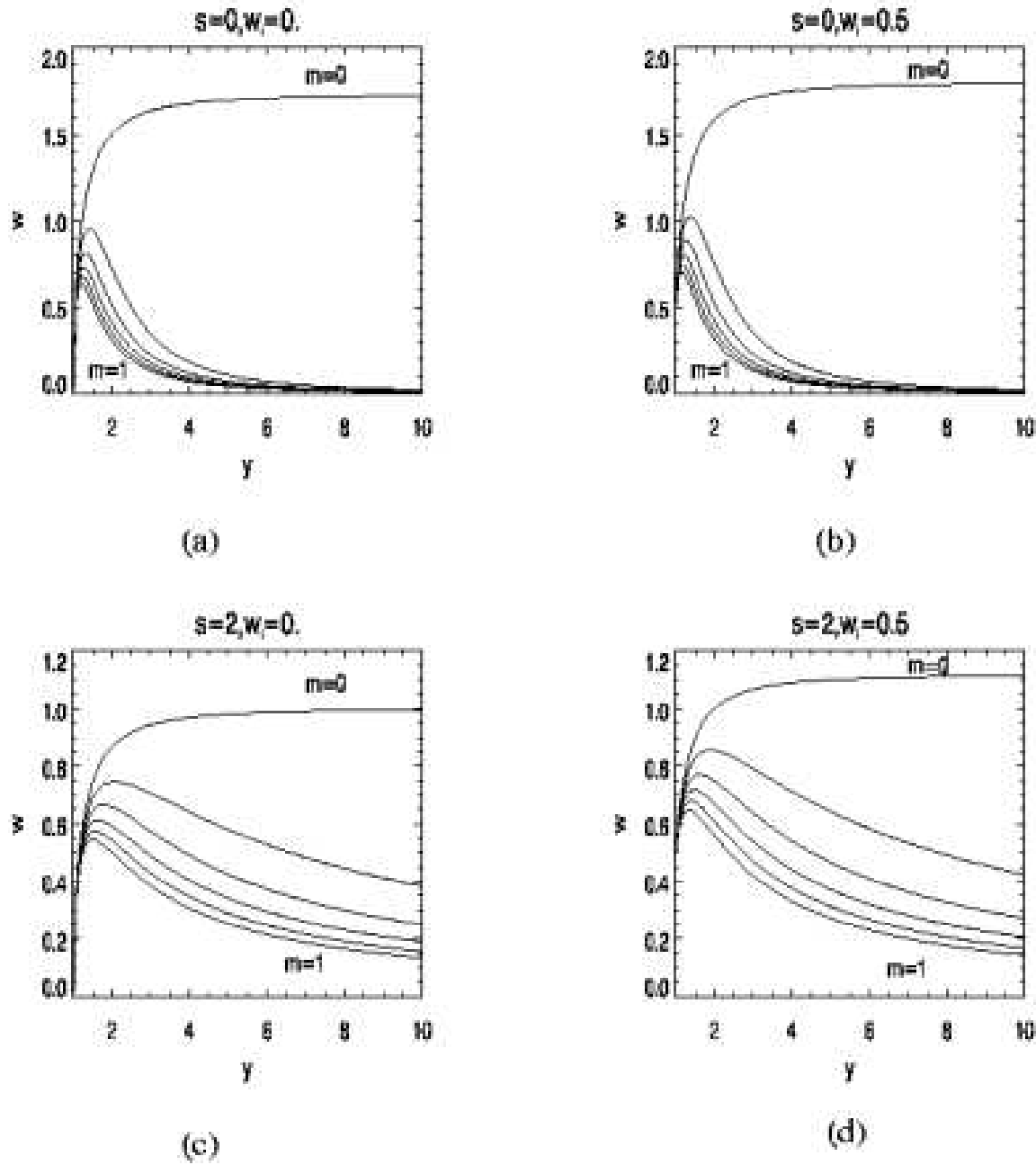


Fig. 3.— The solution for spherical expansion with $s=0$ and $s=2$, for two values of w_i , 0.0 and 0.5. The value of m varies from $m=0$ to $m=1$, in steps of 0.2.

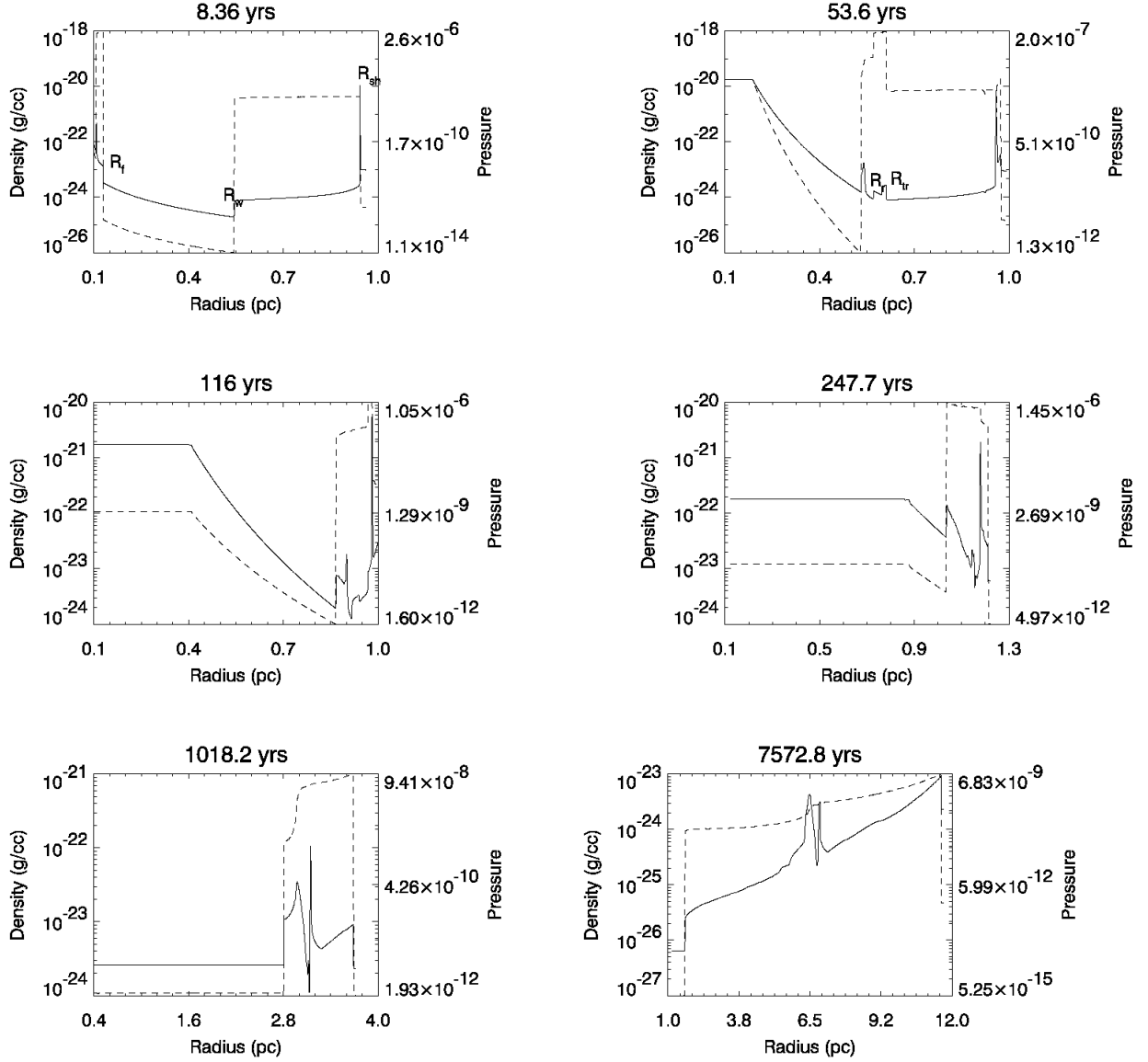


Fig. 4.— Plots showing the density and pressure profile at various times, for the simulation with $\Lambda = 0.14$ Solid line is density, dashed line is pressure. The locations of the SN forward shock (R_f), the wind termination shock (R_w) and the swept up shell R_{sh} are shown in the first frame. Refer to text for other details.

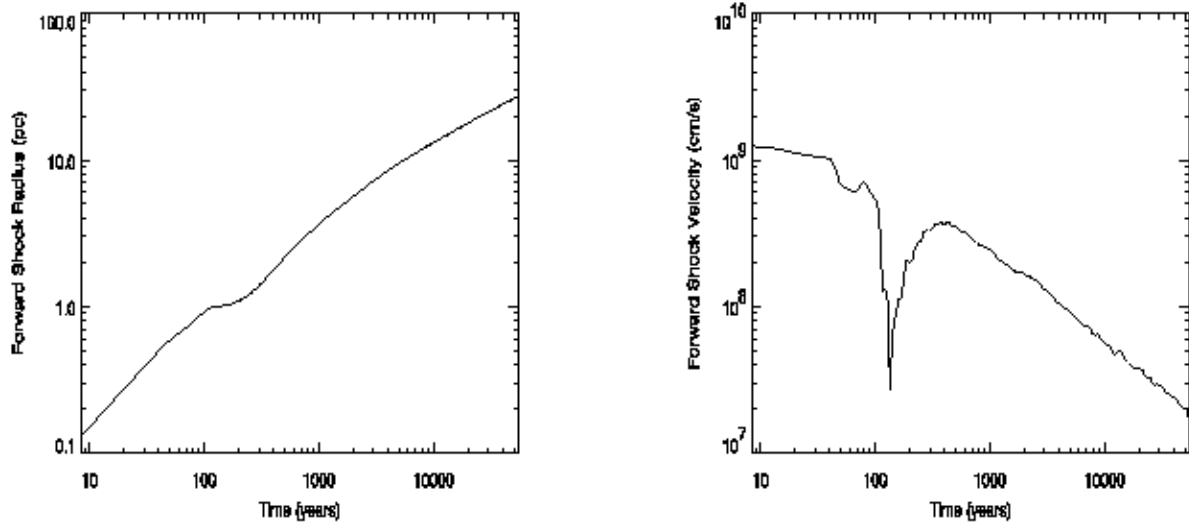


Fig. 5.— Radius(left) and Velocity (right) during the evolution of the SNR for Case 1.

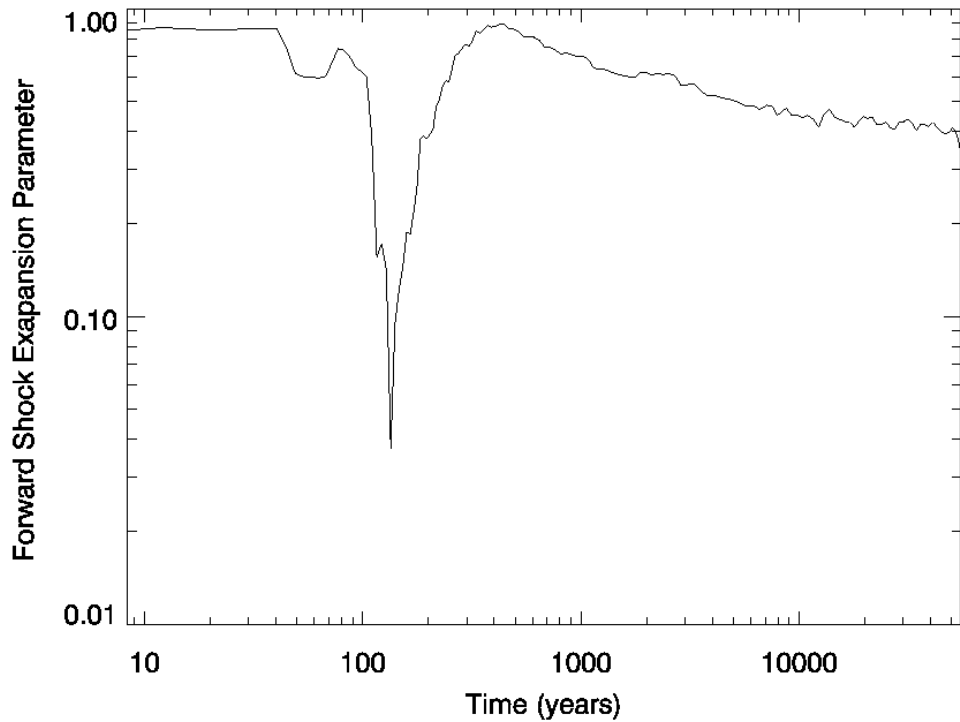


Fig. 6.— The Evolution of the Expansion parameter for Case 1.

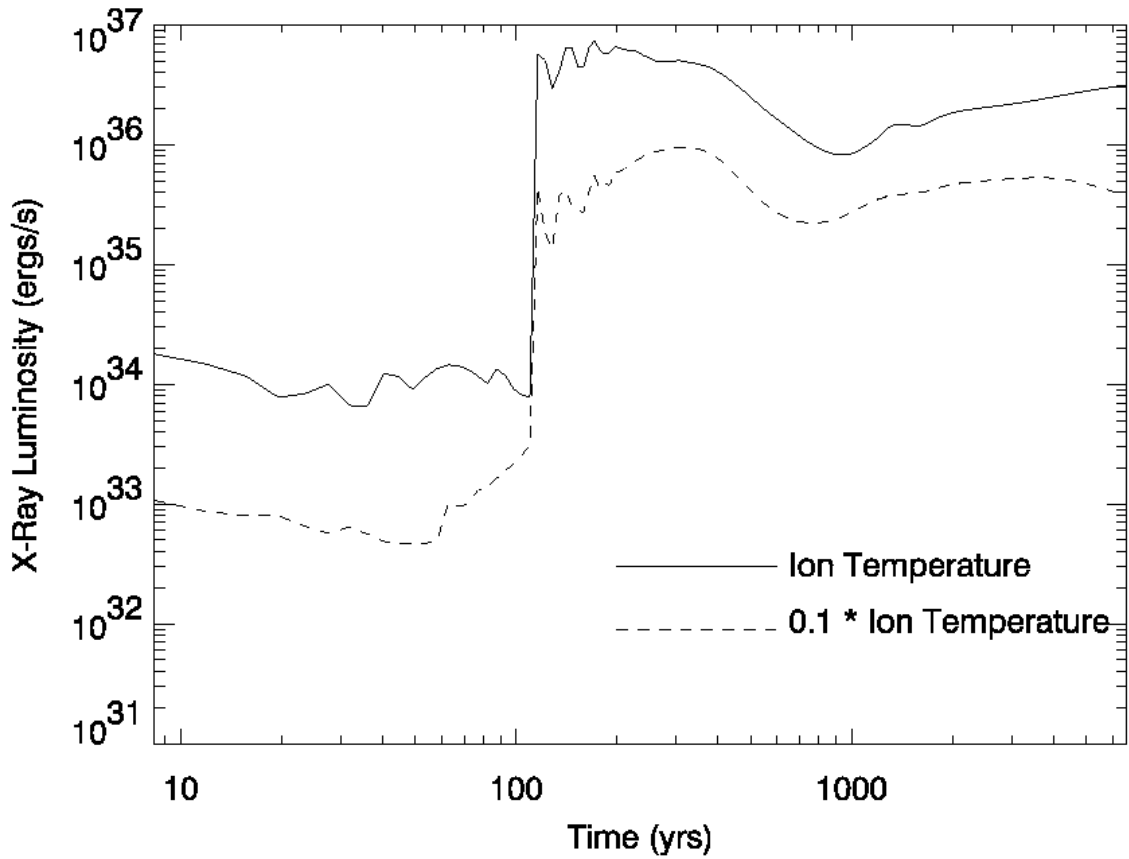


Fig. 7.— The X-ray Luminosity During the Evolution of the remnant in Case 1. Two curves are shown, corresponding to the temperature of the ions within the plasma, and to a value of 10 % of the ion temperature, which is probably more indicative of the electron temperature in the collisionless shock (see text).

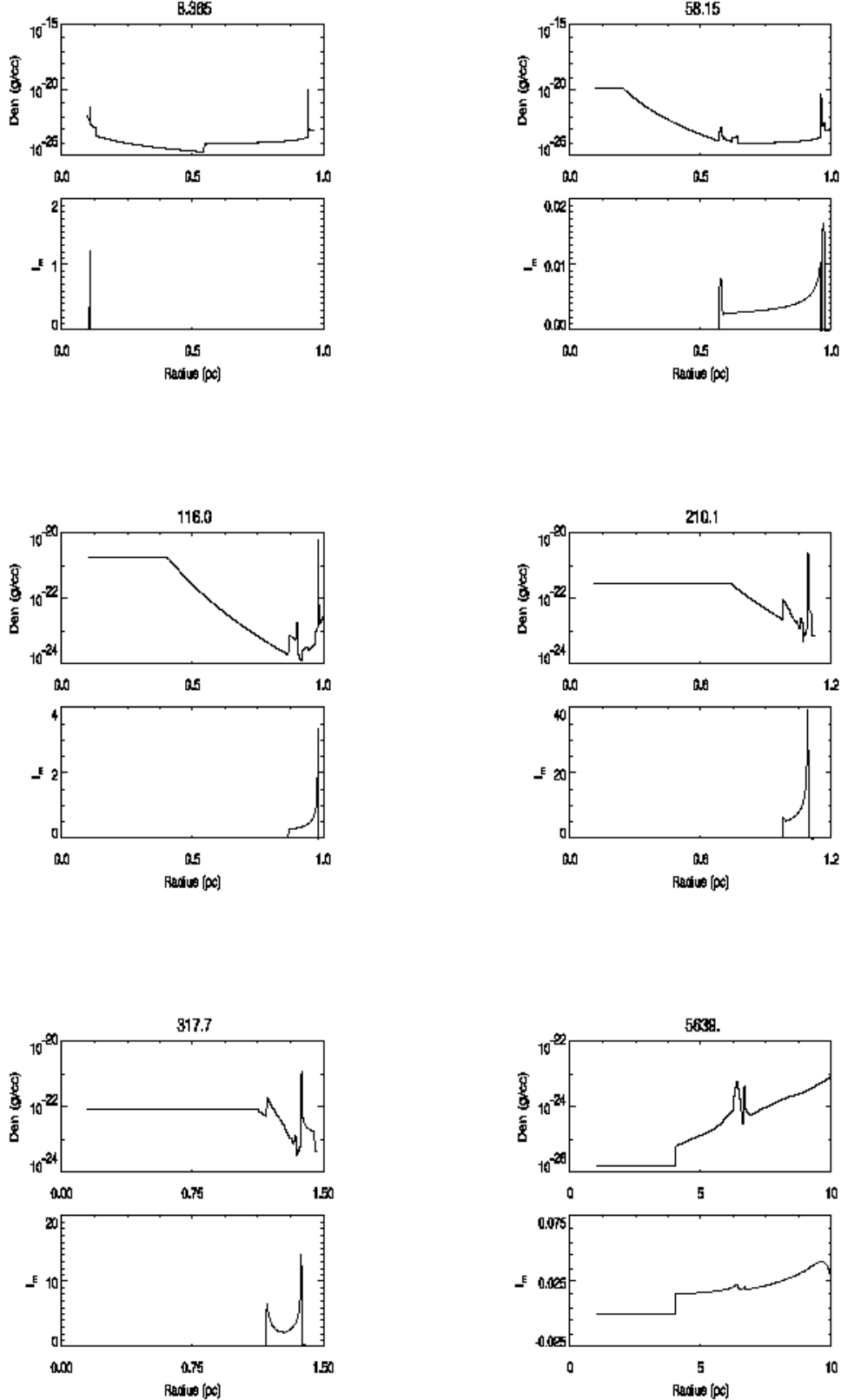


Fig. 8.— Plots showing the evolution of the density (upper panel) and X-ray surface brightness (lower panel) at various times, for the simulation with $\Lambda = 0.14$

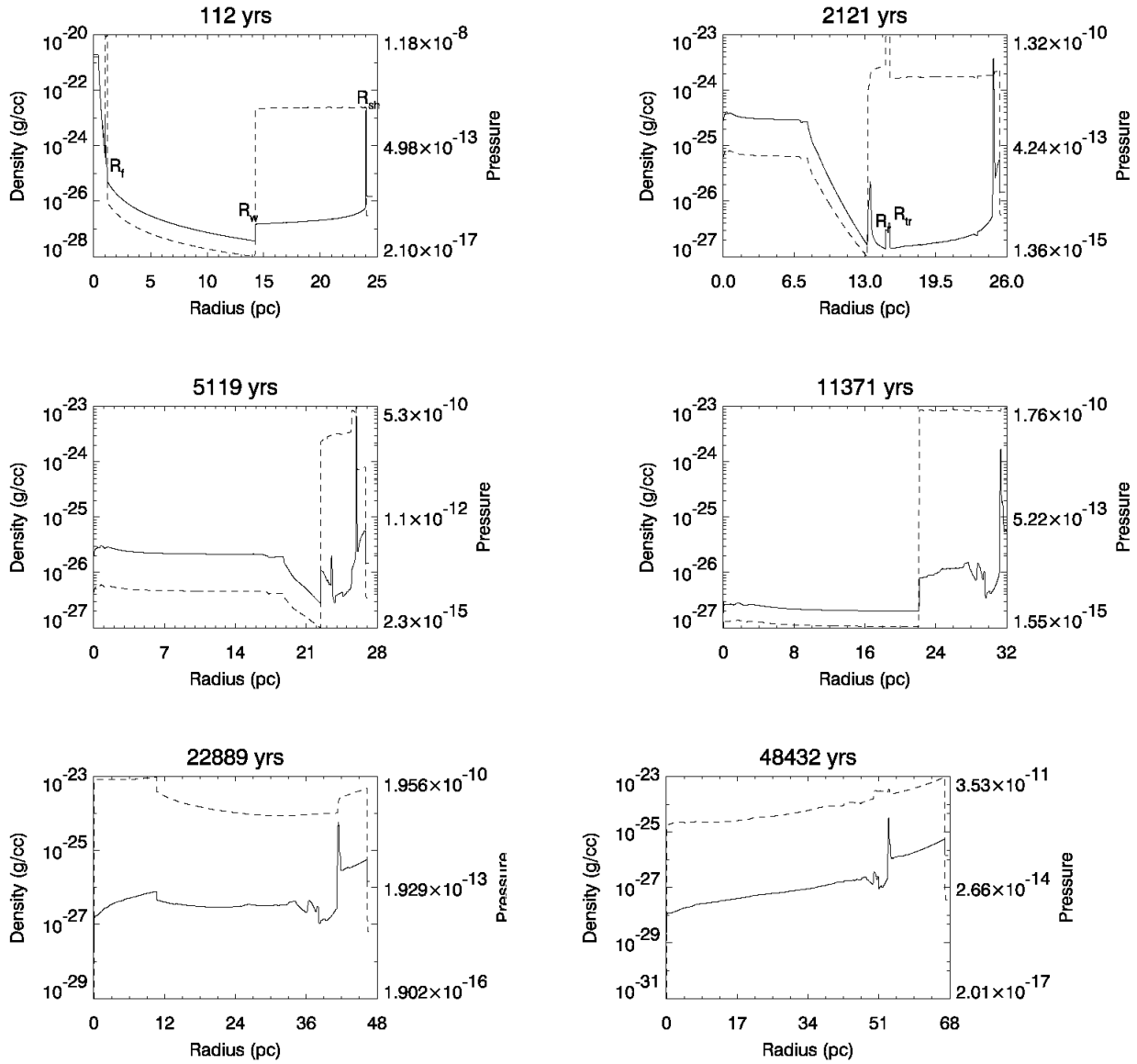


Fig. 9.— Plots showing the density and pressure profile at various times, for the simulation with $\Lambda = 3.7$

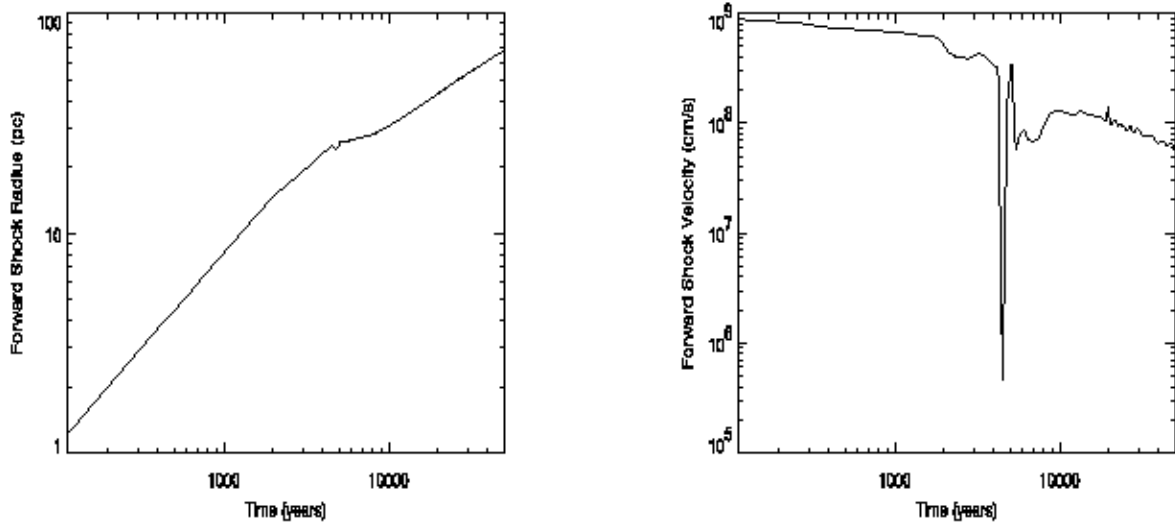


Fig. 10.— Radius (left) and Velocity (right) plots for the evolution of the SNR in Case 2.

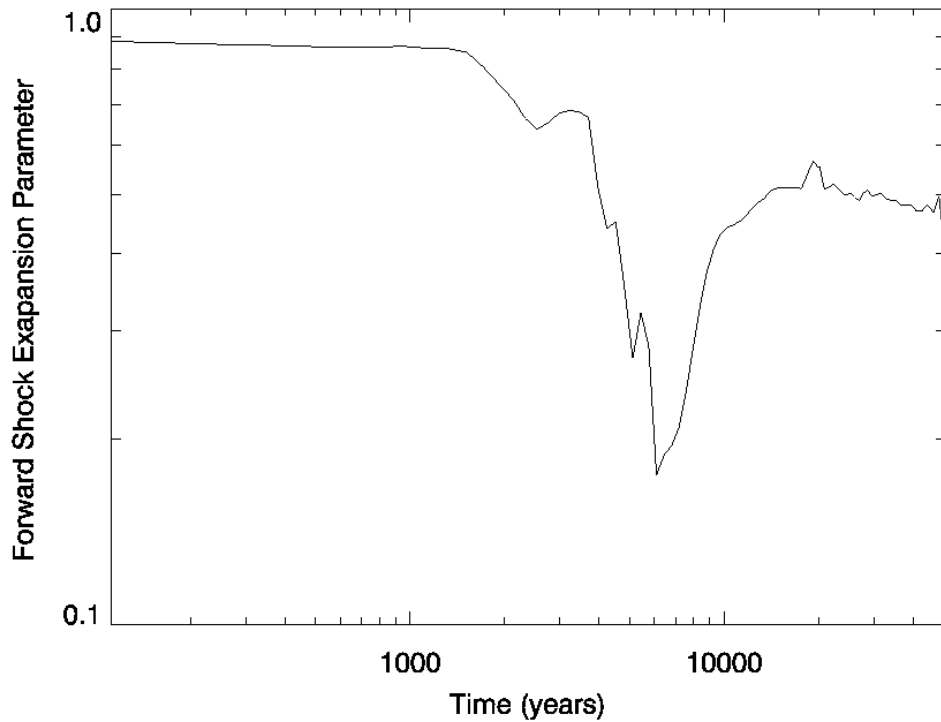


Fig. 11.— The Evolution of the Expansion parameter for Case 2.

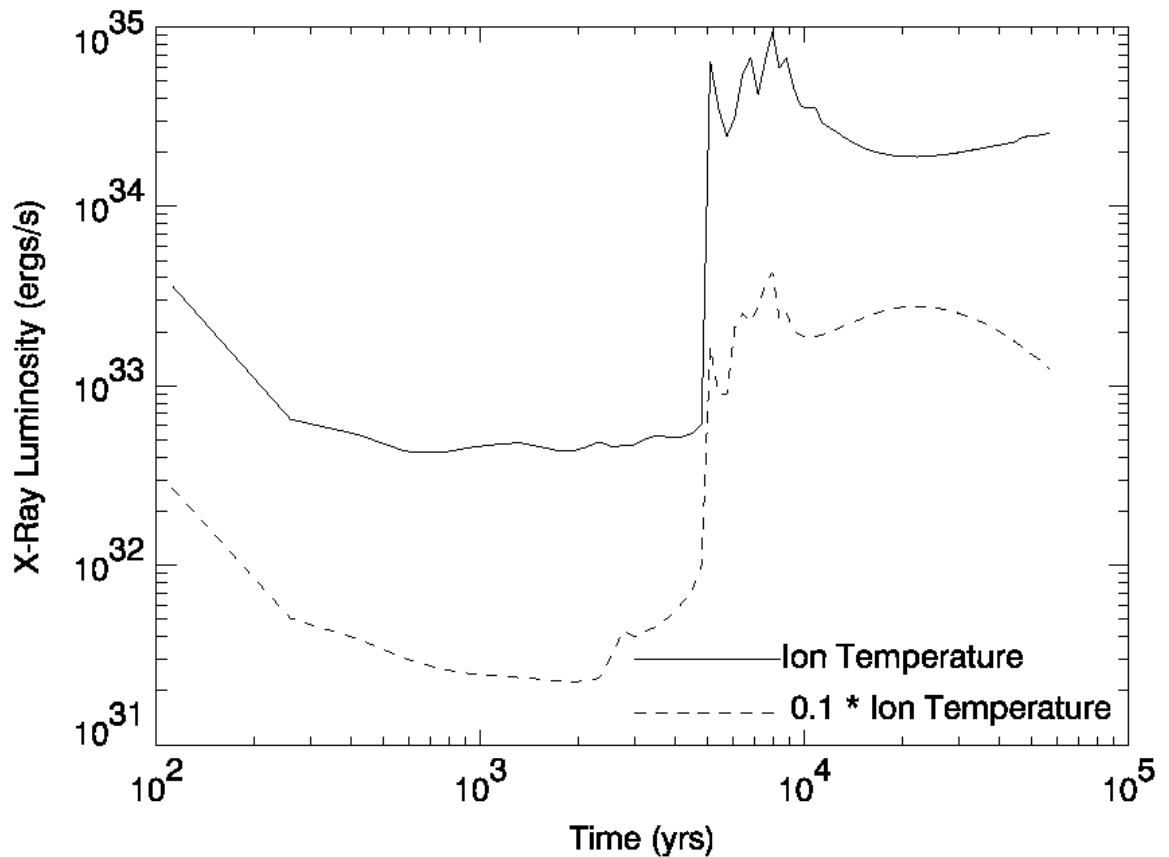


Fig. 12.— The X-ray Luminosity During the Evolution of the remnant in Case 2. For further details see Fig 7.

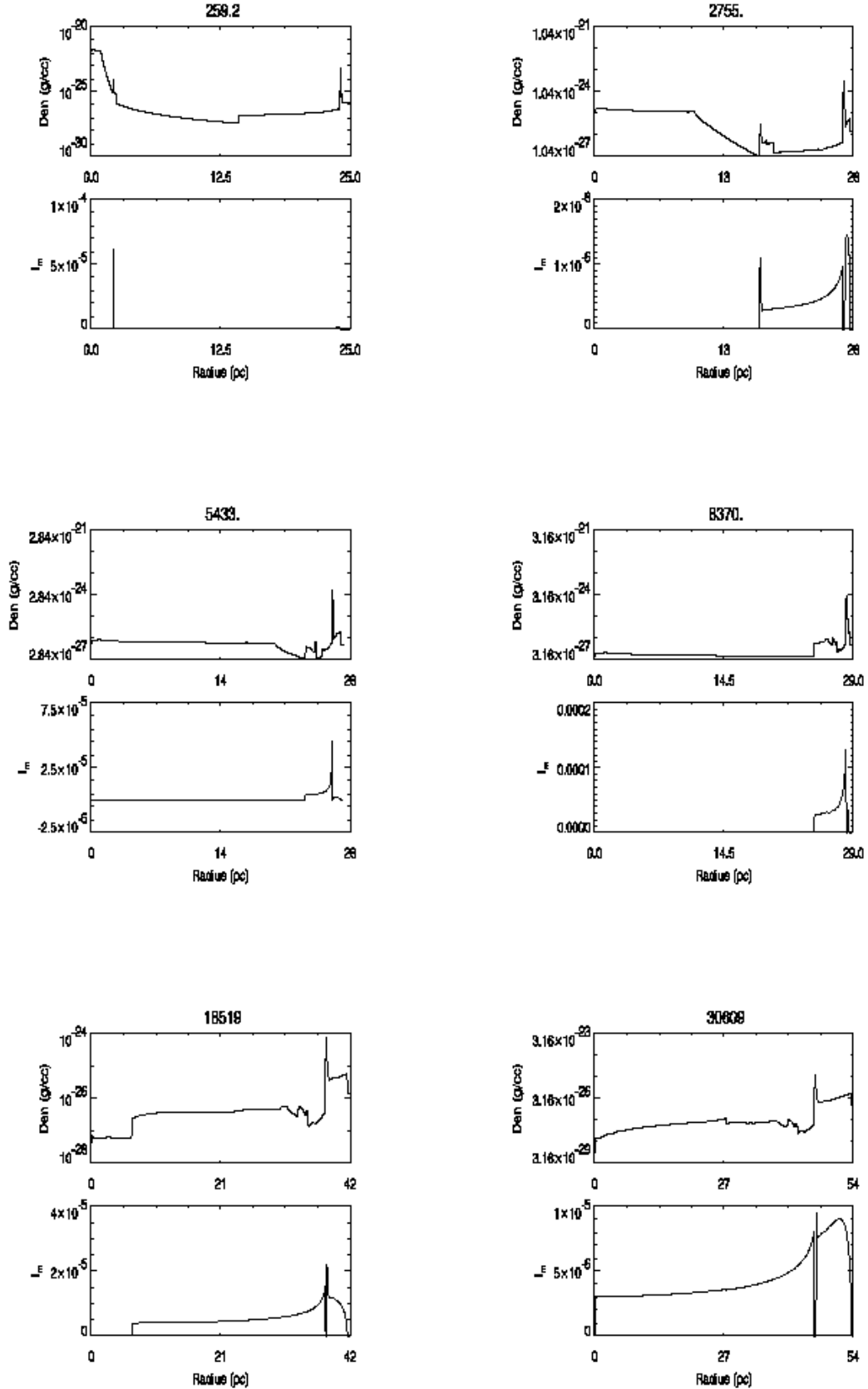


Fig. 13.— X-ray surface brightness profiles during the Evolution of the remnant in Case 2.